

Study on Libration Points of the Sun and the Interstellar Medium for Interstellar Travel

Authors: John Bookless, Colin McInnes

Academic Institution: Department of Aerospace Engineering. University of Glasgow

Approved by: Dario Izzo, Advanced Concepts Team (ESTEC)

Contacts:

Colin McInnes

Tel: ++44 (0)141-330 5918/6143

Fax: ++44 (0)141-330 5560.

e-mail: colinmc@aero.gla.ac.uk

Dario Izzo

Tel: ++31 (0)71565 – 3511

Fax: ++31 (0)71565 – 8018

e-mail: act@esa.int

Ariadna id: 03/4102

Study length: 2 months.

Contract Number: 18140/04/NL/MV

Table of Contents

Executive Summary.....	3
1. Introduction	4
2. Sun-Centauri Libration Point (WP1000)	6
2.1 <i>The Two-Centre Problem.....</i>	6
2.2 <i>Photo-Gravitational Two-Centre Problem</i>	7
2.3 <i>Two-Centre Problem with Relative Motion</i>	10
2.4 <i>Nearby Star Effect on Two-Centre Dynamics.....</i>	12
3. Sun-Galactic Core Libration Point (WP2000).....	21
3.1 <i>Galactic Libration Point Position.....</i>	21
3.2 <i>Halo Orbits about L_1 and L_2.....</i>	22
3.3 <i>Jacobi Integral.....</i>	23
3.4 <i>Transfers Between Interior and Exterior Regions Via L_1 and L_2.....</i>	24
4. Libration Point Transfer for Interstellar Travel (WP3000).....	30
4.1 <i>Two-Centre Transfers.....</i>	30
4.2 <i>Explicit Solution to Two-Centre Problem using Confocal Elliptical Coordinates</i>	31
4.3 <i>Mission Enabling Propulsion Systems</i>	32
5. Summary and Conclusions.....	38
6. References.....	40
Appendix 1.....	42

Executive Summary

A study of possible libration points between the Sun and the nearby Centauri star system has been conducted. The two-centre problem was used to model the gravitational and photo-gravitational dynamics between the two stars, assuming their positions are fixed relative to each other. The aim was to examine the libration point stability and assess the possibility of interstellar matter becoming trapped, at least temporarily, at these points. An unstable on-axis libration point and a range of possible stable and unstable periodic halo-type orbits were identified as a function of the mass to surface area ratio of the test particle.

The validity of the two-centre model was tested by including the gravitational influence of a third star and by introducing the effect of relative motion of Centauri and the Sun. It was found that the relative motion of Centauri and the Sun, of order 30 kms^{-1} , is too fast for particles to become trapped at the libration points due to the long halo-type orbit period, of order 10 Myrs (million years). However, it was demonstrated that stellar motion could perturb the energy of particles, possibly enabling re-capture of escaping particles by the Sun or enabling the escape of bound particles.

A study of libration points between the Sun and the Galactic core was also modeled using Hill's approximation to the circular restricted three-body problem. Assuming the mass of the Galactic bulge to be of order $2 \times 10^{10} \text{ M}_\odot$ (solar masses) and the separation between the Sun and the Galactic core to be 8.5 kpc (kiloparsec), the L_1 and L_2 Lagrange points were located at ± 6.64 ly (light years). Zero-velocity surfaces were examined and a series of possible transits between the interior and exterior Galactic regions were investigated.

Finally, possible transits between the Sun and Centauri were considered. The energy requirements for a fast-flyby mission with a flight time of less than 50 years were compared to a hypothetical long duration transfer via the two-centre libration point. The total energy requirements for the fast-flyby were found to be $+3.142 \times 10^{11} \text{ kJ/kg}$ with a relativistic velocity $0.0873 c$ (speed of light) compared to the energy required using the libration point of -19.776 kJ/kg with a hypothetical mission duration of 30 Myrs. It has been demonstrated that the two-centre model is invalid for long duration missions due to the motion of the Centauri system, so that it does not appear to be possible to exploit the libration point transit. However, a full solution to the two-centre problem for unequal masses was derived by separating the equations using confocal elliptical coordinates. Possible mission enabling propulsion concepts were also investigated with a requirement for high-energy density propulsion technologies.

1. Introduction

The dynamical properties of the libration points of the classical three-body problem are well understood and have been exploited for a range of mission applications, such as libration point halo orbits. More recently, libration points have been seen as a means of enabling low energy transfers between bodies, using the libration points as so-called transit tubes. Such transit tubes appear to offer a means of connecting bodies and providing low energy escape and capture.

A similar analysis can be performed by considering the libration points formed by the Sun and nearby stars. In principle, this is a more complex issue than the classical three-body problem since the nearby stars will form a multi-body problem. In addition, the galactic core provides a gravitational tide which can also form libration points. Such libration points are of interest for a range of applications:

- The libration points formed by the Sun and other stars may provide a region in which interstellar material is (at least temporarily) captured
- The libration points may offer a preferred solar escape trajectory which reduces the energy associated with interstellar travel
- The libration points may offer an interesting target for initial interstellar precursor missions

In this summary report the Sun-Centauri system will be modelled using the classical two-centre problem. The analysis includes an investigation of libration point stability and the effect of photo-gravitational forces due to stellar luminosity. The issue of light extinction will be discussed in order to determine whether photons from nearby stars can exert significant radiation pressure on dust particles at interstellar distances. The effect of the relative motion of the Centauri system and the Sun and the presence of other nearby stars will also be investigated to more accurately model the multi-body dynamics of the local stellar neighbourhood.

The Sun-galactic core system will be considered as a restricted three-body system. The L_1 and L_2 Lagrange points will be identified in the system and possible halo-type orbits around these points will be demonstrated. Using the Jacobi Integral, zero-velocity surfaces will be generated and transfers between the galactic interior and exterior region will be investigated.

The location of L_1 and L_2 will be compared to the position of nearby stars to examine the possible influence of gravitational perturbations on the ideal three-body model.

Finally, transfers between the Sun and Centauri will be examined. Mission energy requirements and timescales will be compared for direct transfers and travel via the two-centre libration points. Finally, mission enabling propulsion options will be investigated for a fast transfer (<50 years) to the Centauri system.

2. Sun-Centauri Libration Point (WP1000)

2.1 The Two-Centre Problem

The dynamics of the Sun-Centauri system will be modelled using the classical two-centre problem. The two-centre problem was first investigated by the Euler in 1790 and may be viewed as a restricting case of the three-body problem.¹ The two-centre problem is a non-rotating system where a particle of negligible mass is moving under the gravitational influence of two fixed masses (or electrostatic influence if fixed charges are considered), see **Figure 2.1.1**.

The Sun and Centauri both revolve around the galactic centre at a distance of order 8.5 kpc (kilo-parsec) from the galactic core. It is assumed that Centauri and the Sun remain at fixed positions relative to each other due to the similar rate of revolution around the galactic core. Ignoring the influence of nearby stars the dynamics can be in principle be modelled as a two-centre problem in polar coordinates using a non-dimensionalised two-centre potential¹

$$\begin{aligned}\ddot{\rho} &= \frac{h_z^2}{\rho^3} - \frac{\rho}{r_1^3} - \frac{\lambda\rho}{r_2^3} \\ \ddot{z} &= -\frac{z}{r_1^3} + \frac{\lambda(1-z)}{r_2^3} \\ \ddot{\theta} &= -\frac{2\dot{\rho}\dot{\theta}}{\rho}\end{aligned}\quad \text{Equation 1}$$

with characteristic length $R=4.36$ ly (separation between Centauri and Sun in light years) and characteristic time $\tau = \sqrt{R^3/GM_1}$. The quantity $h_z = \rho^2\dot{\theta}$ is the z-component of angular momentum where $\dot{\theta} = \sqrt{r_1^{-3} + \lambda r_2^{-3}}$ is the angular velocity of an orbit about the axis of symmetry. G is the gravitational constant, M_1 is the mass of the Sun and $\lambda=M_2/M_1$ is the mass ratio of the Centauri system to the Sun, equal to 2.17. Both stars are positioned on the z-axis and the ρ -axis represents the radial distance from the z-axis. The distance of a test particle from the Sun is $r_1 = \sqrt{\rho^2 + z^2}$ and the distance from Centauri is $r_2 = \sqrt{\rho^2 + (1-z)^2}$.

Libration point stability can be determined by considering the potential energy of the system. A stable orbit corresponds to a local minimum of the potential energy function, while an unstable orbit corresponds to a local maximum or saddle point of the potential energy function. The potential energy function can be defined as

$$U(z, \rho) = \frac{h_z^2}{2\rho^2} - \frac{1}{r_1} - \frac{\lambda}{r_2} \quad \text{Equation 2}$$

with derivatives $U_\rho = -\ddot{\rho}$ and $U_z = -\ddot{z}$. A local minimum of the potential energy function requires $U_{\rho\rho}U_{zz} - U_{\rho z}^2 > 0$, $U_{\rho\rho} > 0$ and $U_{zz} > 0$ to be satisfied. **Figure 2.1.2** shows a contour plot of the potential energy function and **Figure 2.1.3** shows circular orbits corresponding to stable and unstable two-centre orbits about the z-axis.

From **Figure 2.1.2** it is clear that for constant angular momentum there exists three possible nominal orbits. The two orbits near either star are stable, as determined from the local minimum of the potential energy function. These essentially correspond to orbits in the two-body problem with a constant uniform force displacing the particle slightly in the direction of the distant star. The middle orbit is unstable, determined from the saddle point in the potential energy function. There exists a bifurcation dependent on the angular momentum of the problem.¹ If the orbit radius is increased, thus increasing the orbit angular momentum, the number of nominal orbits changes from three to one stable nominal orbit near Centauri. It is found that values of $\rho > 1.75$ ly produce no nominal orbits near the Sun.

2.2 Photo-Gravitational Two-Centre Problem

The effect of stellar luminosity on interstellar matter will now be included in the model resulting in a radiation pressure force. Over the large distances separating stars, interstellar matter absorbs and scatters photons leading to starlight extinction. It must first be determined if stellar luminosity can still exert radiation pressure on dust particles over interstellar distances.

Table 1 contains the spectral details of the Sun and the Centauri system taken from the Nstars database.² Centauri is a triple star system with components A, B and C. A and B are a binary system which orbit each other with a period of 80 years. Their separation varies between an apoapsis of 35 AU and periapsis of 11 AU. Centauri C, also known as Proxima Centauri, is a much smaller red-dwarf possibly orbiting the two larger bodies from a great distance.

Name	Spectral Class	Absolute Mag	Luminosity (W)
Sun	G2-V	+4.77	3.86×10^{26}
α -Centauri A	G2-V	+4.38	5.59×10^{26}
α -Centauri B	K1-V	+5.71	1.16×10^{26}
Proxima	M5.5-V	+15.49	7.41×10^{15}

Table 1 Spectral properties of nearby stars from the NStars database

The lightness number, which represents the ratio of stellar radiation pressure to gravitational attraction is defined as

$$\beta = \frac{L}{4\pi c GM\sigma} \quad \text{Equation 3}$$

where L is the stellar luminosity, M is stellar mass and c is the velocity of light. $\sigma = m/A$ is the loading parameter (areal density) where A is the illuminated surface area and m is the particle mass. If $\beta > 1$, then stellar radiation pressure pushes the particle with greater force than stellar gravity attracts it.³

The luminosity of a star can be calculated from its magnitude. The difference in the magnitude of two stars can be determined by

$$m_1 - m_2 = -2.5 \log_{10} \left(\frac{4\pi d_2^2 L_1}{4\pi d_1^2 L_2} \right) \quad \text{Equation 4}$$

where m_1 and m_2 are the magnitude of the stars, d_1 and d_2 are the distances to the stars and L_1 and L_2 are the stellar luminosities. The absolute magnitude is the magnitude of a star, as seen from a distance of 10 pc (parsec). Centauri A and B are of similar spectral magnitude to the Sun and C is a very dim Red dwarf. Neglecting C, the luminosities of A and B can be combined to give the overall system luminosity of 7.1522×10^{26} W. This is much larger than the solar luminosity of 3.86×10^{26} W.

Photons traversing between stars are subject to absorption and scattering by gaseous atoms/ions and dust grains, collectively known as interstellar matter. In the galactic plane the estimated average extinction value is 1 to 2 magnitudes per 1 kpc pathlength.⁴ Shorter wavelength light is dimmed to a greater extent by scattering and absorption than longer wavelength light, thus there is a reddening of starlight which increases systematically with distance.^{5,6} **Figure 2.2.1** shows the percentage reduction in apparent stellar luminosity when

starlight extinction is taken into account. Over the relatively short distance of 4.36 ly for Centauri, the reduction is only 0.12%. Using this assumption, the conclusion is that stellar radiation pressure will still play an important role in the dynamics between the Sun and Centauri.

The gravitational, on-axis two-centre libration point between the two stars is located 1.76 ly from the Sun and 2.59 ly from Centauri. The luminosity of the Sun and Centauri at this libration point are reduced by 0.05% and 0.07% respectively. In the case of the Sun, $\beta > 1$ requires $\sigma < 7.672 \times 10^{-4} \text{ kgm}^{-2}$. In the case of Centauri, the combined luminosity requires $\sigma < 6.549 \times 10^{-4} \text{ kgm}^{-2}$ for $\beta > 1$. The non-dimensionalised equations of motion including photo-gravitational terms are

$$\ddot{\rho} = \frac{h_z^2}{\rho^3} - \frac{(1-\beta_1)\rho}{r_1^3} - \frac{\lambda(1-\beta_2)\rho}{r_2^3}$$

$$\ddot{z} = -\frac{(1-\beta_1)z}{r_1^3} + \frac{\lambda(1-\beta_2)(1-z)}{r_2^3}$$

Equation 5

where β_1 and β_2 represent the lightness number for the Sun and Centauri respectively.

We can consider the effect that stellar radiation pressure has on the position of the libration point. For the values of luminosity of the Sun and Centauri, we find that $\beta_1 > \beta_2$ regardless of the test particle size, due to the larger mass of Centauri. **Figure 2.2.2** represents the possible values of ρ and z , which could accommodate orbiting test particles of varying areal density. We now consider three cases:

$\beta_2 < \beta_1 < 1$: In this case stellar gravity is still the dominant force. For particles with $\sigma = 3 \times 10^{-3} \text{ kgm}^{-2}$, the lightness number values are small and possible orbit values of ρ and z are not displaced significantly from the values when radiation pressure forces are ignored. As σ decreases the on-axis libration point position moves towards the Sun and the bifurcation radius decreases until $\sigma < 7.672 \times 10^{-4} \text{ kgm}^{-2}$. This is due to the effective mass of the Sun, as seen by a particle, being reduced by a factor $(1-\beta_1)/(1-\beta_2)$.

$\beta_2 < 1 < \beta_1$: Between areal densities of $6.549 \times 10^{-4} < \sigma < 7.672 \times 10^{-4} \text{ kgm}^{-2}$ there exists a scenario where there are no available orbits to trap particles between the two stars. In this case the dominant force from the Sun is solar radiation pressure, and the dominant force from Centauri is gravity. Particles are pushed away from

the Sun and are attracted toward Centauri (provided the particle velocity does not exceed the effective escape speed).

From **Figure 2.2.2**, contour 2 indicates there are possible orbits for z-axis positions $z < 0$ and $z > 1$. The required angular velocity is given by $\dot{\theta} = \sqrt{(1 - \beta_1)/r_1^3 + \lambda(1 - \beta_2)/r_2^3}$, which must be a real number in order to obtain a real orbit. As $\beta_1 > 1$, $(1 - \beta_1) < 0$ and conversely $(1 - \beta_2) > 0$. Thus, it is required that the first term under the square root is less than the second. Near the Sun $r_2 \gg r_1$ so the angular velocity is imaginary meaning that orbits with $z < 0$ cannot exist. Near Centauri $r_1 \gg r_2$ so we have a real value for angular velocity. Orbits with $z > 4.36$ ly do exist and are unstable, as determined using eigenvalue analysis.

$\beta_1 > \beta_2 > 1$: In this case the dominant force is radiation pressure and orbits can no longer be obtained as the combined radiation pressure will push any particles out of the system. Interestingly, when $(1 - \beta_1) > \lambda(1 - \beta_2)$ the effective mass of Centauri is less than the Sun so the on-axis libration point lies nearer Centauri than the Sun. The on-axis libration point is unstable and any motion off-axis will cause the particle to be swept from the system due to radiation pressure.

The possible off-axis orbits, in which a particle can become trapped are determined from the test particle areal density. After a thorough investigation, it was found that particles with $\sigma > 3 \times 10^{-3}$ kgm⁻², can only remain trapped in orbits corresponding to the radius and z-axis location mapped along contour 5 of **Figure 2.2.2**. Smaller particles can reside in orbits corresponding to successive contours between contour 5 and 3. For particles with $\sigma < 6.549 \times 10^{-4}$ kgm⁻² there will be no orbits in which these particles can remain trapped. This analysis has defined the types of particles we may expect to find trapped between the Sun and Centauri. Now, we must take into account the relative motion of Centauri to the Sun.

2.3 Two-Centre Problem with Relative Motion

The two-centre approximation is only valid if the period of orbits about the z-axis is short in comparison to the relative motion of Centauri to the Sun. The orbit period is in the order of 1×10^7 years. From the Gliese catalogue⁷ the relative radial velocity of Centauri A to the Sun is -26.2 kms⁻¹ with a proper motion of 3.689 arcsec/yr corresponding to $V_x = -26.2$ kms⁻¹ and $V_y = 23.39$ kms⁻¹.

Over a relatively short time period (<1000 years) the star positions can be approximated as stationary, but over millions of years this assumption is clearly no longer valid. **Figure 2.3.1**

shows the motion of the Centauri system relative to the Sun. Also plotted is the relative motion of the libration point between the stars. It can be calculated that the libration point position must move with velocity components $v_{xL}=-10.44 \text{ km s}^{-1}$ and $v_{yL}=9.32 \text{ km s}^{-1}$.

Figure 2.3.2 shows the effect of Centauri motion on an unstable orbit about the z-axis. In this case the initial conditions define an unstable orbit around a libration point. The radiation pressure effects have been included for a dust grain with areal density $\sigma=3\times10^{-3} \text{ kg m}^{-2}$. In this case $0<\beta_1<1$ and $0<\beta_2<1$, so the dominating force acting on the particle is gravity from both stars. The dynamics are modelled using the following equations, where the Sun and Centauri lie on the x-axis and the axis orientation is chosen such that the motion of Centauri relative to the Sun is in the x-y plane with respective velocity components v_x and v_y so that

$$\begin{aligned}\ddot{x} &= -\frac{x(1-\beta_1)}{r_1^3} + \frac{\lambda(1-\beta_2)(1+v_x t - x)}{r_2^3} \\ \ddot{y} &= -\frac{y(1-\beta_1)}{r_1^3} + \frac{\lambda(1-\beta_2)(v_y t - y)}{r_2^3} \\ \ddot{z} &= -\frac{z(1-\beta_1)}{r_1^3} - \frac{\lambda(1-\beta_2)z}{r_2^3}\end{aligned}\quad \text{Equation 6}$$

where $r_2 = \sqrt{(1+v_x t - x)^2 + (v_y t - y)^2 + z^2}$.

A test particle behaves as though the gravitational attraction of Centauri is not present and the result is an apparent two-body problem between the test particle and the Sun. The reason for this is the relative motion of the particle compared to the stars. A particle moving slowly relative to the Sun is moving at roughly 30 km s^{-1} relative to Centauri, well in excess of the required escape velocity from these distances. If the particle has the initial velocity and direction of the Centauri system, again there exists a two-body scenario and the particle is bound to the potential-well of Centauri (provided the relative velocity is less than the escape velocity).

There is a small perturbation introduced to a particle bound to the Sun as Centauri moves within the vicinity of the Sun. When the particle is far from the Sun (~ 1 ly), the passing Centauri system introduces a perturbation of order 1 ms^{-1} to the test particle velocity components. The size of this perturbation decreases if the particle is initially closer to the Sun and increases if the particle is initially closer to Centauri. **Figure 2.3.3** shows an interesting case comparing the two-body problem to the two-centre problem with relative stellar motion. A particle with the minimum required solar escape velocity could be recaptured by the Sun due to passing near Centauri. Relative to Centauri, the particle is well in excess of the escape velocity and so will not be captured by the star. However, as the particle passes Centauri its velocity is decreased by about 30 ms^{-1} . At this distance, the

kinetic energy reduction could be enough to cause the particle to return to the Sun in a very highly elliptical orbit. **Figure 2.3.4** shows the resulting elliptical orbit with a period of 480 Myrs compared to the two-body escape trajectory.

This study has shown that the two-centre libration point orbits are unlikely to exist, due to the relatively fast velocity of nearby stars relative to the Sun. **Table 2** shows the velocity of a few nearby stars relative to the Sun, extracted from the Gliese catalogue.

Star	Dist (ly)	Radial vel (kms ⁻¹)	Proper Motion (arcsec/yr)	v _x (kms ⁻¹)	v _y (kms ⁻¹)
α-Centauri A	4.36	-26.2	3.689	-26.2	23.39
α-Centauri B	4.36	-18.1	3.689	-18.1	23.39
Proxima	4.22	-16.0	3.809	-16.0	23.38
Sirius	8.58	-9.4	1.328	-9.4	16.57
Barnards Star	5.96	-111.0	10.31	-111.0	89.37

Table 2 Local stellar velocities relative to the Sun

All nearby stars to the Sun move at relatively high velocities. The red-dwarf Barnard's star is moving at an impressive 142.5 kms⁻¹ relative to the Sun. At these velocities, and due to the long time required for orbits around the libration points which exist between the stars (~ 10 Myrs) it is concluded that in most cases the two-centre problem would not be an applicable model for local stellar dynamics.

2.4 Nearby Star Effect on Two-Centre Dynamics

Another case to be considered is when the gravitational influence of other nearby stars are included in the two-centre model. Sirius is a binary system, one of the brightest stars in the sky and is at a distance of 8.58 ly from the Sun. The larger Sirius A is twice as massive as the Sun and has a luminosity of 8.0647×10^{27} W. Sirius B is a much smaller, but extremely heavy white dwarf with a mass similar to the Sun's compressed into a volume 90% of the Earth.⁸ The total mass of the Sirius system is 3.2 M (solar masses), and the effective luminosity due to 1 mag/kpc light extinction leads to a luminosity reduction of only 0.26%. Again, the reference point is the on-axis libration point between the Sun and Centauri, which is at a distance of 9.55 ly from Sirius. The extinction corrected luminosity for Sirius at this distance corresponds to a reduction of only 0.27%.

The coordinate system is orientated such that the Sun and Centauri are positioned on the x-axis and the x-y plane is chosen such that all three stars are coplanar. Adding the additional

photo-gravitational terms for a third star positioned at (X,Y,Z), the two-centre equations can be written as

$$\begin{aligned}\ddot{x} &= -\frac{x(1-\beta_1)}{r_1^3} + \frac{\lambda_1(1-\beta_2)(1-x)}{r_2^3} + \frac{\lambda_2(1-\beta_3)(X-x)}{r_3^3} \\ \ddot{y} &= -\frac{y(1-\beta_1)}{r_1^3} - \frac{\lambda_1(1-\beta_2)y}{r_2^3} + \frac{\lambda_2(1-\beta_3)(Y-y)}{r_3^3} \\ \ddot{z} &= -\frac{z(1-\beta_1)}{r_1^3} - \frac{\lambda_1(1-\beta_2)z}{r_2^3} + \frac{\lambda_2(1-\beta_3)(Z-z)}{r_3^3}\end{aligned}\quad \text{Equation 7}$$

where λ_1 is the mass ratio of the Centauri System to the Sun and λ_2 is the mass ratio of Sirius to the Sun equivalent to 2.17 and 3.2 respectively. The lightness number β_3 represents the ratio of radiation pressure to gravitational attraction acting on a test particle due to Sirius. The distance of the test particle from Sirius is $r_3 = \sqrt{(X-x)^2 + (Y-y)^2 + (Z-z)^2}$. The Cartesian position of Sirius and Centauri relative to the Sun are provided in **Table 3**.

Star	Right Ascension (h m s)	Declination (d m s)	X (ly)	Y (ly)	Z (ly)
a-Centauri A	14 39 36.5	-60 50 2	-1.630	-1.363	-3.807
a-Centauri B	14 39 35.1	-60 50 13	-1.630	-1.363	-3.807
Proxima	14 29 43.0	-62 40 46	-1.538	-1.177	-3.736
Sirius	06 45 08.9	-16 42 58	-1.608	8.058	2.468

Table 3 Stellar positions relative to Sun at origin

The coordinate system is orientated so that all stars lie in the Z=0 plane. The coordinates of the three stars become Sun (0,0,0), α -Centauri (1,0,0) and Sirius (-0.942,-1.728,0) where the characteristic length is, as before $L=4.36$ ly. The potential energy function can be defined as

$$U(x, y, z) = -\frac{(1-\beta_1)}{r_1} - \frac{\lambda_1(1-\beta_2)}{r_2} - \frac{\lambda_2(1-\beta_3)}{r_3} \quad \text{Equation 8}$$

We now consider three different particle parameters to examine the following lightness number cases:

$\beta_2 < \beta_1 < \beta_3 < 1$: **Figure 2.4.1** shows the potential energy contours for a particle with areal density $\sigma=1\times10^{-2}$ kgm⁻². These particles would have a lightness number

$\beta_1=0.0767$ $\beta_2=0.0655$ $\beta_3=0.4998$. The dominant force acting on these particles would be the gravity from all three stars. There are two libration points in this plane, one between Centauri and the Sun and one between these stars and Sirius. Both of these points are unstable, as determined from the saddle point in the potential energy function.

$\beta_2 < \beta_1 < 1 < \beta_3$: **Figure 2.4.2** shows the case when particle areal density is $\sigma=3 \times 10^{-3} \text{ kgm}^{-2}$. The lightness number values would be $\beta_1=0.2557$ $\beta_2=0.2183$ $\beta_3=1.6659$. In this case the dominant force exerted by Sirius is stellar radiation pressure, while the other stars both have dominant gravitational forces. Particles corresponding to these lightness numbers are pushed away from Sirius and those which do not exceed the escape velocity of the Sun or Centauri, could become trapped within these star's potential wells.

$\beta_2 < \beta_1 < 1 \sim \beta_3$: **Figure 2.4.3** shows the case for particles with loading parameter $\sigma=5 \times 10^{-3} \text{ kgm}^{-2}$. The lightness values would be $\beta_1=0.1534$ $\beta_2=0.1310$ $\beta_3=0.9996$. As the lightness number due to Sirius is almost 1, stellar radiation pressure almost exactly cancels the gravitational force. There is still a saddle point in the potential function between the Sun and Centauri, but the potential well due to Sirius has vanished as it no longer influences the particle motion.

In conclusion, the position of the libration point varies, dependant on the lightness number of the test particle being considered. Again, the libration point position will move due to the motion of the stars, which will reduce the possibility of dust becoming temporarily trapped between the stars.

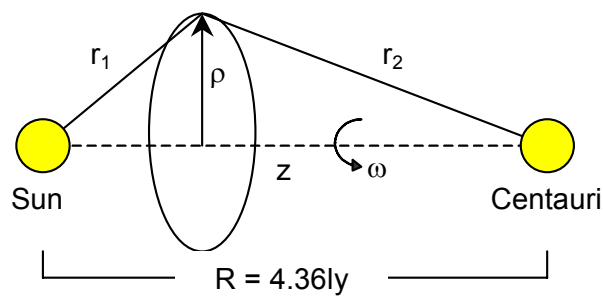


Figure 2.1.1 Two-Centre Model

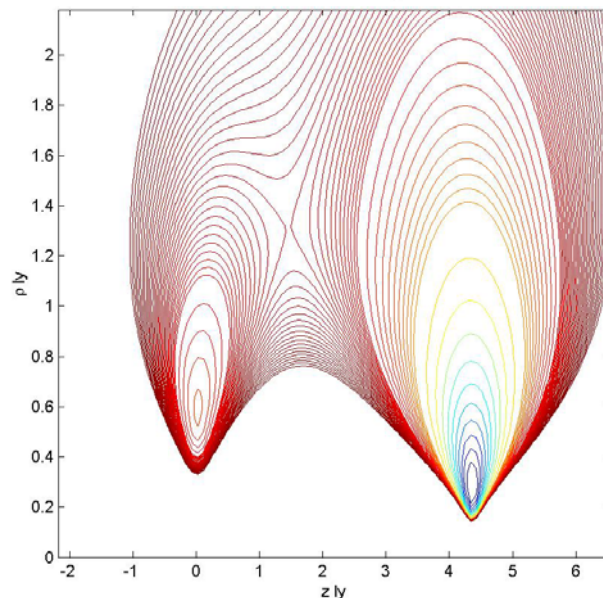


Figure 2.1.2 Two-Centre Potential Energy Function $h_z=0.3673$

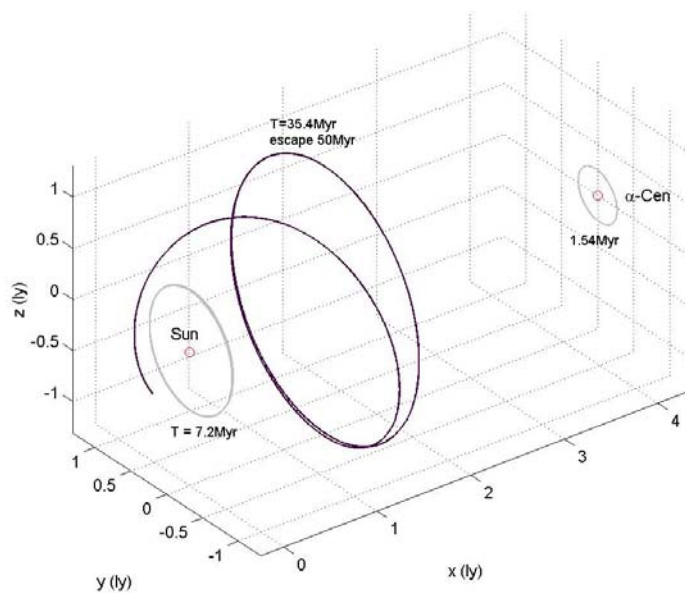


Figure 2.1.3 Two-Centre Stable and Unstable Orbits

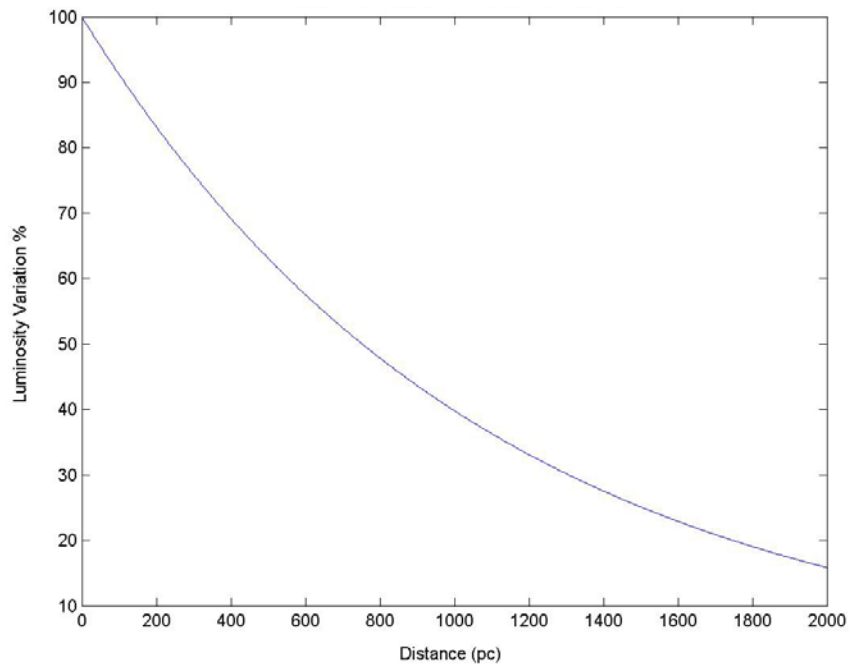
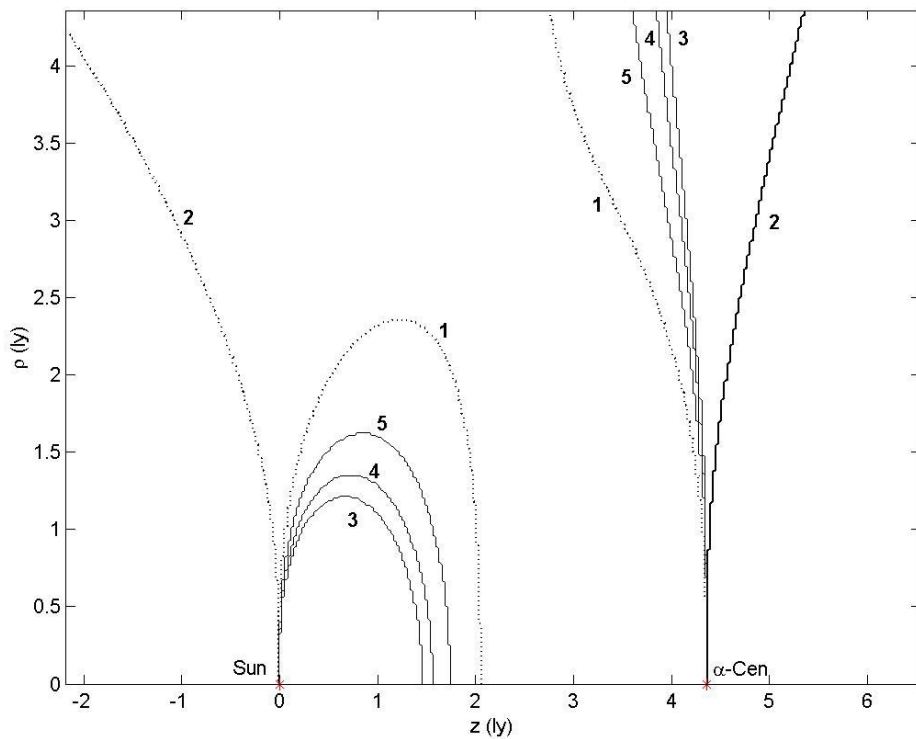


Figure 2.2.1 Light extinction varying as separation distance



Values of σ (kgm^{-2}) contours: **1**= 5×10^{-4} **2**= 7×10^{-4} **3**= 9×10^{-4} **4**= 1×10^{-3} **5**= 3×10^{-3}

Figure 2.2.2 Possible orbit ρ - z values for different particle loading values
**dotted-line corresponds to imaginary angular velocity so orbit cannot exist*

Libration Points of the Sun and Interstellar Medium

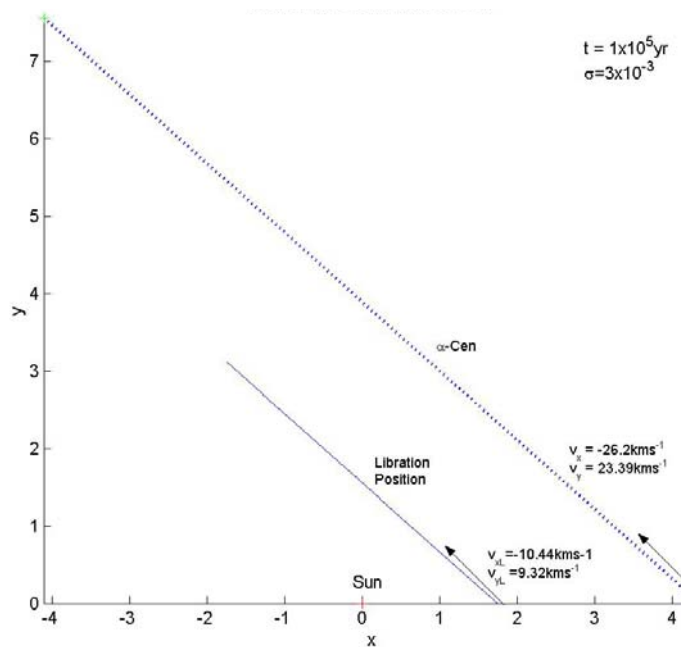


Figure 2.3.1 Motion of Centauri and Libration point relative to the Sun

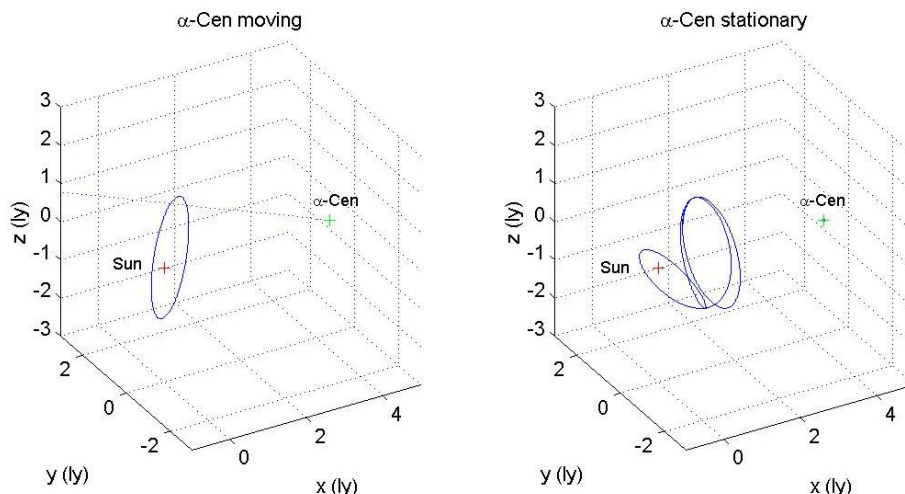


Figure 2.3.2 Effect of Centauri motion on dust particle trajectories

Libration Points of the Sun and Interstellar Medium

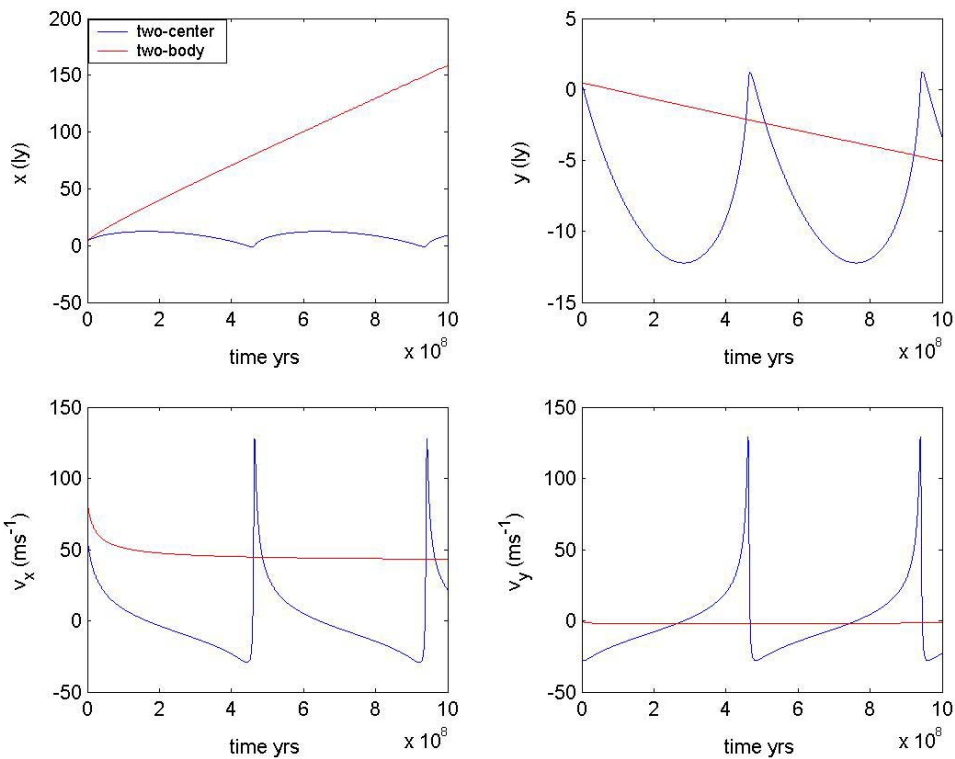


Figure 2.3.3 Effect of relative motion of Centauri on particle position and velocity

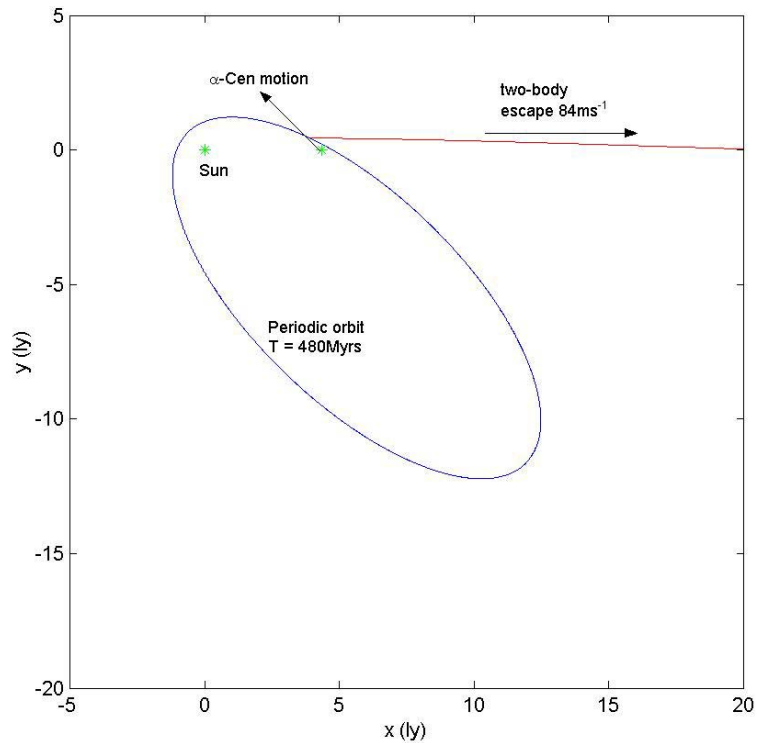


Figure 2.3.4 Solar particle capture due to kinetic energy reduction

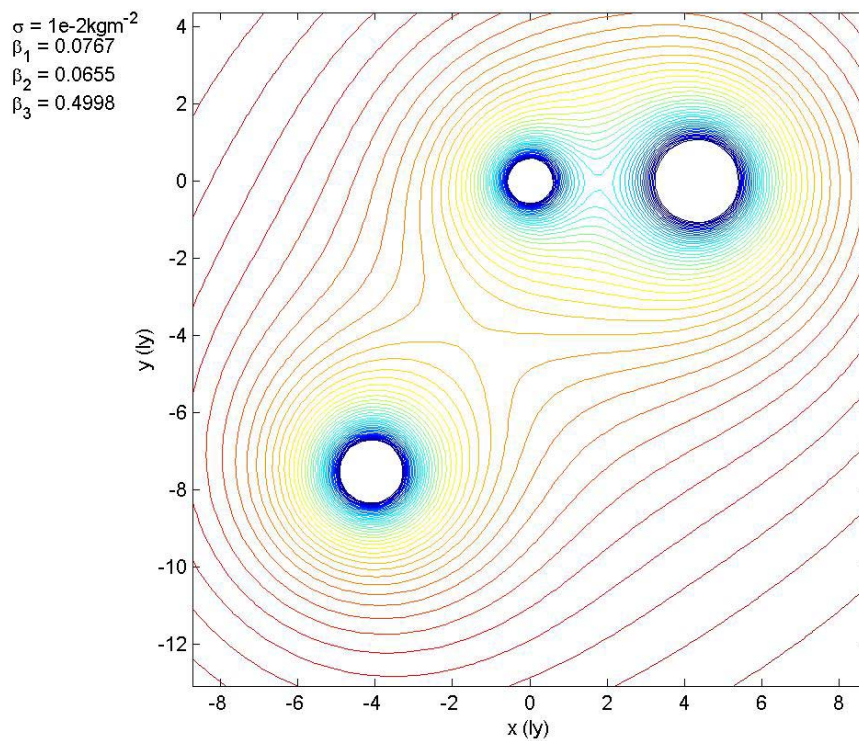


Figure 2.4.1 Libration point between Sun-Centauri-Sirius for particle $\sigma=1\times 10^{-2}\text{kgm}^{-2}$

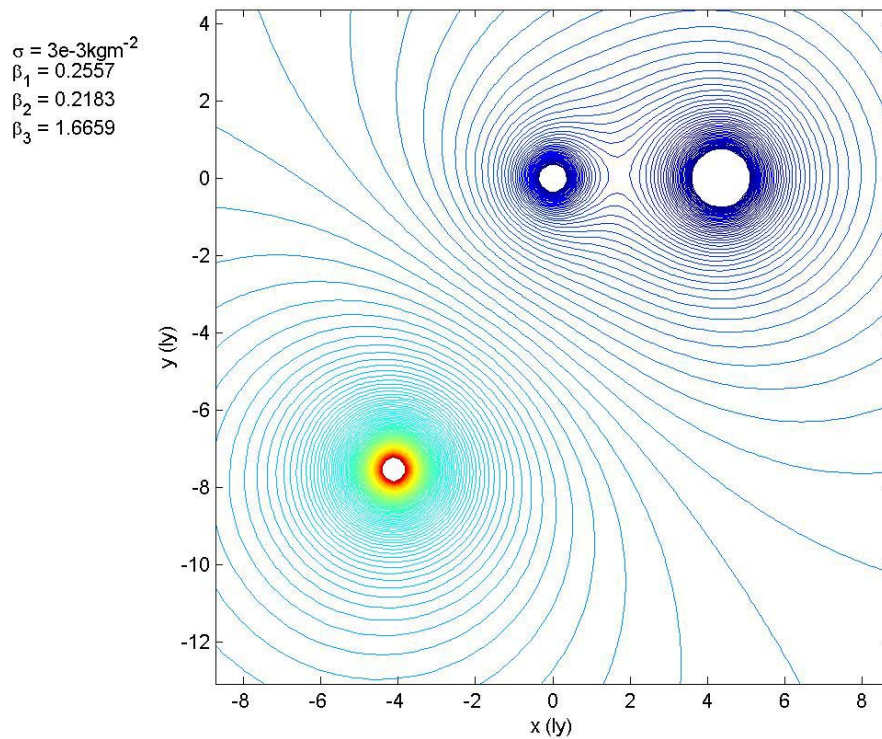


Figure 2.4.2 Libration point between Sun-Centauri-Sirius for particle $\sigma=3\times 10^{-3}\text{kgm}^{-2}$

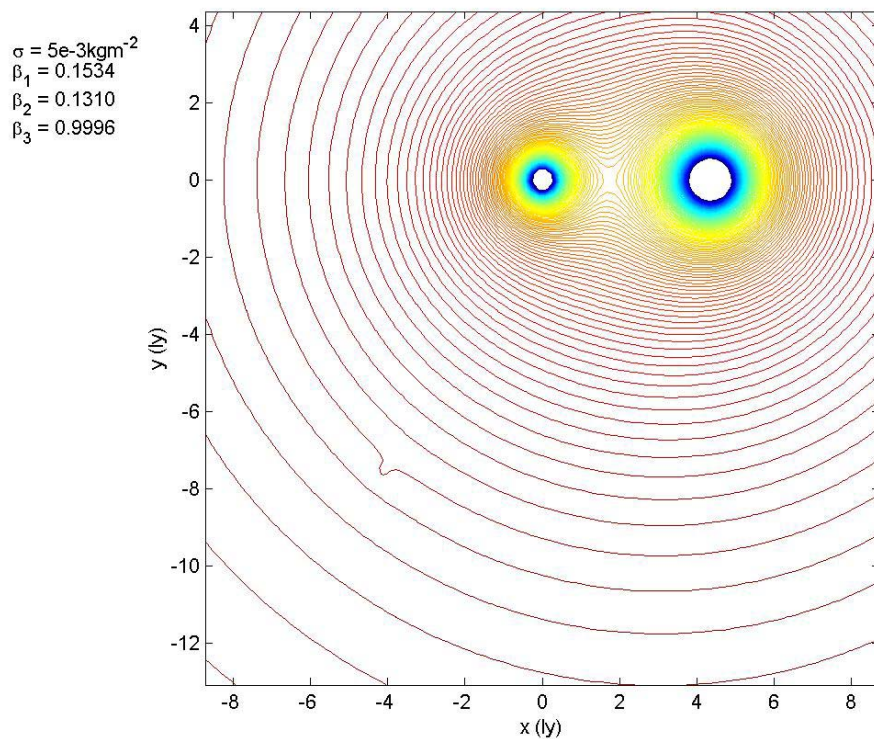


Figure 2.4.3 Libration point between Sun-Centauri-Sirius for particle $\sigma=5 \times 10^{-3} \text{ kgm}^{-2}$

3. Sun-Galactic Core Libration Point (WP2000)

3.1 Galactic Libration Point Position

In recent years, several missions have made use of invariant manifolds which exist in the rotating three-body problem - including the NASA/ESA ISEE-3/ICE 1978,⁹ the Japanese Hiten 1991,¹⁰ NASA WIND 1994 (Interplanetary Physics Laboratory)¹¹ and the ESA/NASA SOHO 1995 (Solar and Heliospheric Observatory).¹² Advantages of using the manifold tubes when developing spacecraft trajectories are the lower mission energy requirements than more conventional trajectories.

The dynamics of the solar system orbiting the centre of the galaxy can be modelled as a three-body problem. The Milky-Way galaxy is considered to be a barred-spiral galaxy. The Sun is located approximately 8.5 kpc (26,000 ly) from the centre of the galaxy, a value estimated using the very bright variable stars in the globular clusters located in the galactic halo. The mass of the galactic bulge has recent estimates ranging between $1 \times 10^{10} M_{\odot}$ (solar masses) to $2 \times 10^{10} M_{\odot}$.^{13,14,15} The latter will be accepted as the galactic bulge mass.

Hill's approximation of the three-body problem will be used to model the Sun orbiting the galactic core. This model assumes perfectly circular motion and that the larger primary mass is fixed at the centre, as opposed to both primaries orbiting a barycentre. The effect of stellar radiation pressure from the bulge stars can be ignored as over a distance of 8.5 kpc there is a reduction in luminosity of over 99%. The non-dimensionalised Hill's equations are defined as

$$\begin{aligned}\ddot{x} - 2\Omega\dot{y} &= -\frac{x}{r^3} + 3\Omega^2 x \\ \ddot{y} + 2\Omega\dot{x} &= -\frac{y}{r^3} \quad \text{Equation 9} \\ \ddot{z} &= -\frac{z}{r^3} - \Omega^2 z\end{aligned}$$

where Ω is the non-dimensionalised angular velocity of the Sun orbiting the Galactic centre and $r = \sqrt{x^2 + y^2 + z^2}$ is the distance of a test particle from the Sun. The coordinate system is orientated such that the Sun and the Galactic centre are positioned along the x-axis with the galactic centre in the -x direction, while the y-axis is in the direction of solar motion. The equations are non-dimensionalised with characteristic length $L = 1$ ly (light-year) and characteristic time $\tau = \sqrt{L^3/\mu_s}$ where μ_s is the solar gravitational parameter. The angular

velocity of the Sun orbiting the Galactic centre is defined as $\Omega = \sqrt{\mu_g / R^3}$, where R is the distance between the Galactic centre and the Sun, and the Galactic centre gravitational parameter is $\mu_g = 1.334 \times 10^{30} \text{ m}^3 \text{s}^{-2}$. This gives a value for the Galactic orbit period of 470 Myrs.

To identify the position of the L_1 and L_2 libration points we set all acceleration and velocity terms equal to zero and as the libration points lie on the x -axis, $z=y=0$ also. This reduces the equations to give $x = \pm \sqrt[3]{1/3\Omega^2}$, which corresponds to $x = \pm 6.6413$ ly. L_2 is positioned on the $+x$ -axis (anti-Galactic direction) and L_1 is positioned on the $-x$ -axis.

3.2 Halo Orbits about L_1 and L_2

Having located the position of the on-axis libration points, their stability can be investigated and initial conditions that lead to quasi-periodic halo orbits identified. From **Equation 9**, it is clear that the x and y equations are coupled. A 4x4 stability matrix can be employed to examine the stability of these equations. **Equation 9** can be re-written in the form

$$\begin{aligned}\ddot{x} - 2\Omega\dot{y} &= -U_x \\ \ddot{y} + 2\Omega\dot{x} &= -U_y \\ \ddot{z} &= -U_z\end{aligned}\quad \text{Equation 10}$$

where $U_x = x/r^3 - 3\Omega^2$, $U_y = y/r^3$ and $U_z = z/r^3 + \Omega^2 z$ are pseudo-potentials which can be differentiated in order to linearise the equations of motion. The linearised equations may then be represented as a matrix with variable $X = [x, y, \dot{x}, \dot{y}]^T$ so that

$$\dot{X} = \begin{bmatrix} 0 & 0 & 1 & 0 \\ 0 & 0 & 0 & 1 \\ -U_{xx} & -U_{xy} & 0 & 2\Omega \\ -U_{yx} & -U_{yy} & -2\Omega & 0 \end{bmatrix} \quad \text{Equation 11}$$

The equations are linearised about the L_2 point, giving $U_{xx} = -0.01024$, $U_{xy} = 0$, $U_{yx} = 0$ and $U_{yy} = 0.00341$. The eigenvalues, λ_i and corresponding eigenvectors can be extracted from the stability matrix to obtain $\lambda_{1,2} = \pm 0.084612$ and $\lambda_{3,4} = \pm 0.069881i$. Since there is one positive real eigenvalue, it can be deduced that the libration point is unstable. The imaginary eigenvalues represent oscillatory motion, so selecting certain initial conditions can temporarily dampen the effect of the real eigenvalues using the following method. Firstly, we write the solution to the linearised equations of motion as

$$\begin{aligned}
 x &= \alpha_1 \xi_1 \exp(\lambda_1 t) + \alpha_2 \xi_2 \exp(\lambda_2 t) + \alpha_3 \xi_3 \exp(\lambda_3 t) + \alpha_4 \xi_4 \exp(\lambda_4 t) \\
 y &= \alpha_1 \eta_1 \exp(\lambda_1 t) + \alpha_2 \eta_2 \exp(\lambda_2 t) + \alpha_3 \eta_3 \exp(\lambda_3 t) + \alpha_4 \eta_4 \exp(\lambda_4 t) \\
 \dot{x} &= \alpha_1 \xi_1 \lambda_1 \exp(\lambda_1 t) + \alpha_2 \xi_2 \lambda_2 \exp(\lambda_2 t) + \alpha_3 \xi_3 \lambda_3 \exp(\lambda_3 t) + \alpha_4 \xi_4 \lambda_4 \exp(\lambda_4 t) \\
 \dot{y} &= \alpha_1 \eta_1 \lambda_1 \exp(\lambda_1 t) + \alpha_2 \eta_2 \lambda_2 \exp(\lambda_2 t) + \alpha_3 \eta_3 \lambda_3 \exp(\lambda_3 t) + \alpha_4 \eta_4 \lambda_4 \exp(\lambda_4 t)
 \end{aligned}
 \tag{Equation 12}$$

where ξ_i and η_i represent the eigenvectors for the eigenvalue λ_i , and α_i are constant coefficients where $i=\{1,2,3,4\}$. To dampen the real eigenvalue terms, we set the constants $\alpha_1=\alpha_2=0$ and calculate the resulting initial conditions at $t=0$. **Figure 3.2.1** shows an orbit about the L_2 libration point with a radius of 10 Mkm and period of 227 Myrs. For this halo orbit the initial conditions are $x_0=6.6413$ ly, $\dot{x}=2.7342 \times 10^{-6}$ ms $^{-1}$, $y_0=1 \times 10^{10}$ m, $\dot{y}=0$ and the required z-components can be calculated as $z_0=0$, $\dot{z}=im\{\lambda_3\}$, $y_0=8.7713 \times 10^{-6}$ ms $^{-1}$. A similar halo orbit can be positioned around the L_1 libration point, provided in **Figure 3.2.2**. The total orbital energy will now be investigated as means of determining long-term stability.

3.3 Jacobi Integral

Due to the assumption of a constant angular rotation rate of the Sun orbiting the Galactic centre, a Jacobi integral can be extracted from Hill's equations.^{16,17} The integral represents the total orbit energy as

$$C = v^2 - \frac{2}{r} - \Omega^2 (3x^2 - z^2) \tag{Equation 13}$$

where C is known as the Jacobi constant, which is equivalent to twice the total energy while v represents the test particle velocity. By calculating the value of C for a set of initial conditions the contours can be examined for $v=0$. These contours mark out a zero-velocity surface for constant energy.

Figure 3.3.1 shows a set of zero-velocity surfaces in the Galactic plane for values of $C=\{-0.3, -0.4, -0.45, -0.5\}$. As energy is increased the zero-velocity surface gradually opens about the L_1 and L_2 libration points. Energy corresponding to an open zero-velocity surface allows transfers between the interior and exterior regions.¹⁸ A closed zero-velocity surface forbids transfers and can hold trapped particles in the vicinity of the Sun.

Before utilising the L_1 and L_2 points as a means of low energy transfers, nearby stars will be investigated which may be in the vicinity of the libration points. The galactic centre is positioned in the constellation Sagittarius (Sgr A*) at a position defined by Right Ascension 17h 45m 40s and Declination 29° 00m 28s. **Figure 3.3.2** marks out the 11 stars within 3 pc

of the Sun and the position of the Galactic L_1 and L_2 libration points. **Table 4** shows for each of the stars the radial distance from L_1 and L_2 .

Star name	Distance from Sun (ly)	Distance from L_1 (ly)	Distance from L_2 (ly)
Luyten 726-8A	8.72	13.49	7.64
Luyten 726-8B	8.72	13.49	7.64
Sirius A	8.58	15.01	3.20
Sirius B	8.58	15.01	3.20
Wolf 359	7.78	10.85	9.57
Lalande 21185	8.29	9.79	11.40
α -Centauri A	4.36	8.33	7.51
α -Centauri B	4.36	8.33	7.54
Proxima	4.22	8.39	7.31
Barnard's Star	5.96	2.75	12.32
Ross 154	9.68	7.83	14.64

Table 4 All stars within 3pc of Sun distance from L_1 and L_2

The red-dwarf Barnard's Star is 2.75 ly from the L_1 libration point, although with an estimated mass of $0.17 M_\odot$ probably has little effect on the zero-velocity surface shape. The large binary system Sirius is presently only 3.2 ly from the L_2 libration point. As the Sun orbits the galactic centre and the other stars change position relative to the Sun and the Galactic libration points, other stars may pass near to these libration points which could alter the shape of the zero-velocity surface.

3.4 Transfers Between Interior and Exterior Regions Via L_1 and L_2

Dust particles could be transferred from the interior Galactic region to the exterior Galactic region provided their energy corresponds to an open zero-velocity surface. **Figure 3.4.1** shows a particle transfer via the L_1 and L_2 libration points. The Jacobi Constant value $C=-0.4401$, which is equivalent to a total energy $E=-1.4233$ kJ/kg. The particle direction is perturbed slightly as it passes L_1 and is temporarily bound within the zero velocity surfaces performing two passes around the Sun before escaping into the exterior region.

If the total energy is less, the opening of the zero-velocity surface is reduced thus decreasing the possibility of capture from the interior or exterior region. **Figure 3.4.2** represents a particle from the Galactic interior region approaching the L_1 libration point. It performs a

quasi-periodic lissajous orbit around the libration point but the particle is rejected by the capture region and remains in the interior galactic region.¹⁸ The Jacobi constant $C=-0.4430$, which is equivalent to a total energy $E= -3.1233$ kJ/kg.

If the total energy corresponds to a closed zero-velocity surface then particles within the capture region will remain bound to the Sun and conversely, particles in the interior and exterior will remain in their respective regions. **Figure 3.4.3** shows an example of this where $C=-0.4824$, which is equivalent to $E=-3.4011$ kJ/kg. Also examined was a case where particles from the interior region have enough energy to pass into the capture region but do not quickly escape, shown in **Figure 3.4.4**, where this surface has an energy $E=-3.1608$ kJ/kg.

The Jacobi integral energy analysis allows prediction of the probable motion of particles with a certain total energy moving within the interior, capture and exterior region. However, other considerations can affect the shape of the zero-velocity surface for a particular particle. Stellar radiation pressure from the Sun and other nearby stars can alter the forces acting on a particle. Also, as demonstrated in the two-centre analysis (Section 2), the passing of nearby stars can perturb the motion of a particle thus altering its total energy.

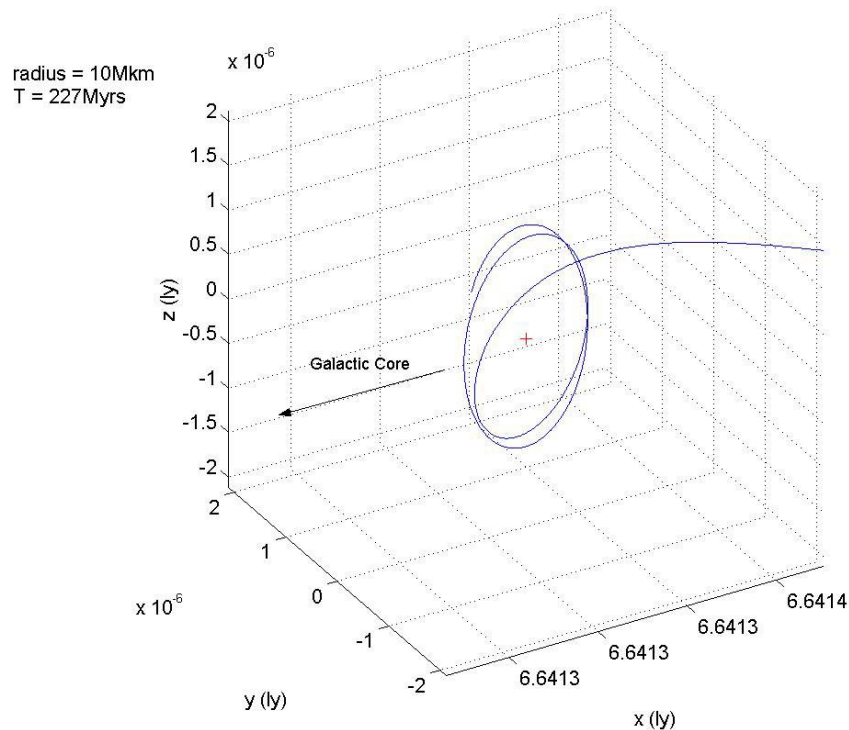


Figure 3.2.1 Halo orbit around Galactic L_2 libration point

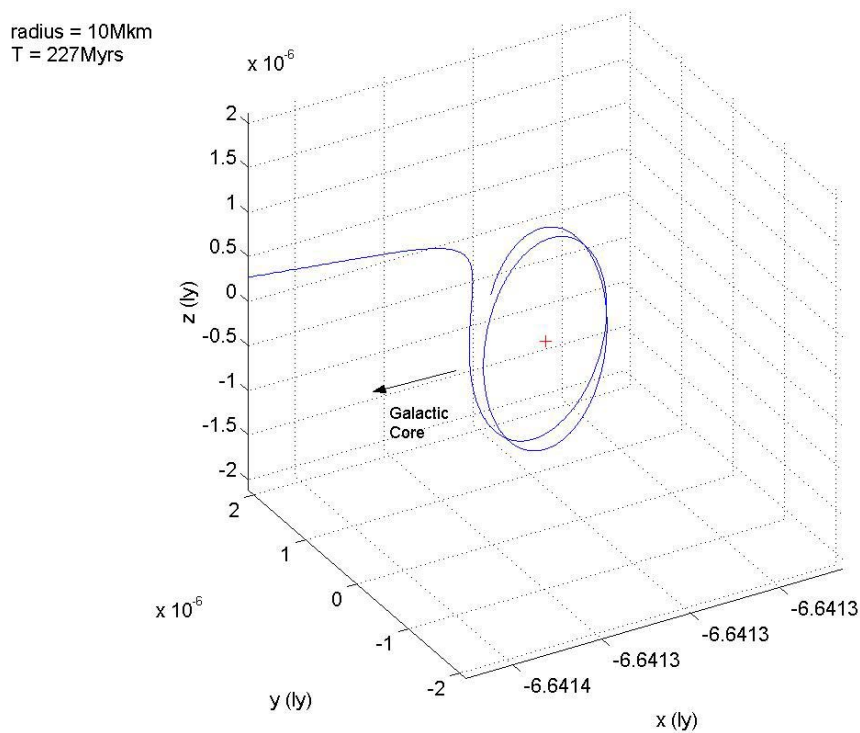


Figure 3.2.2 Halo orbit around Galactic L_1 libration point

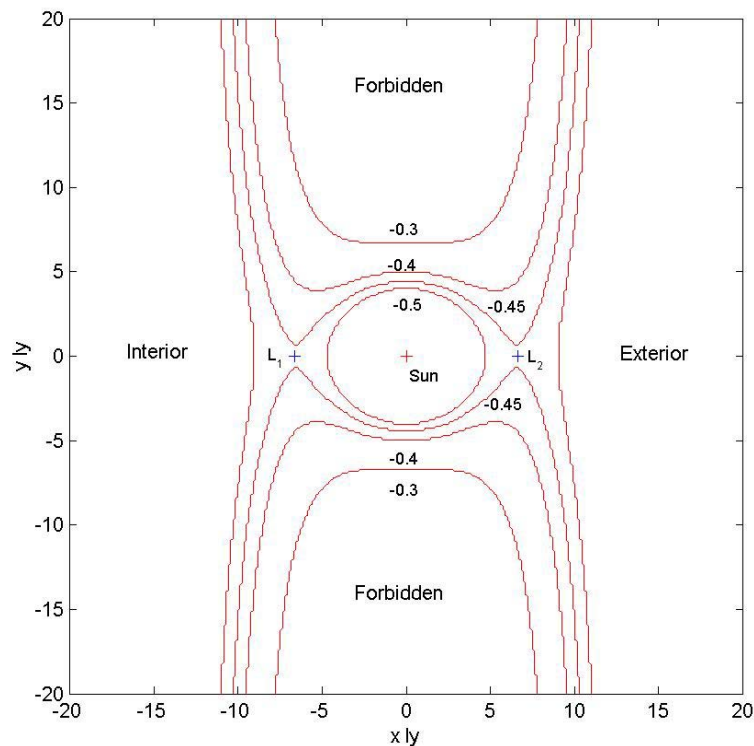


Figure 3.3.1 Zero velocity surfaces

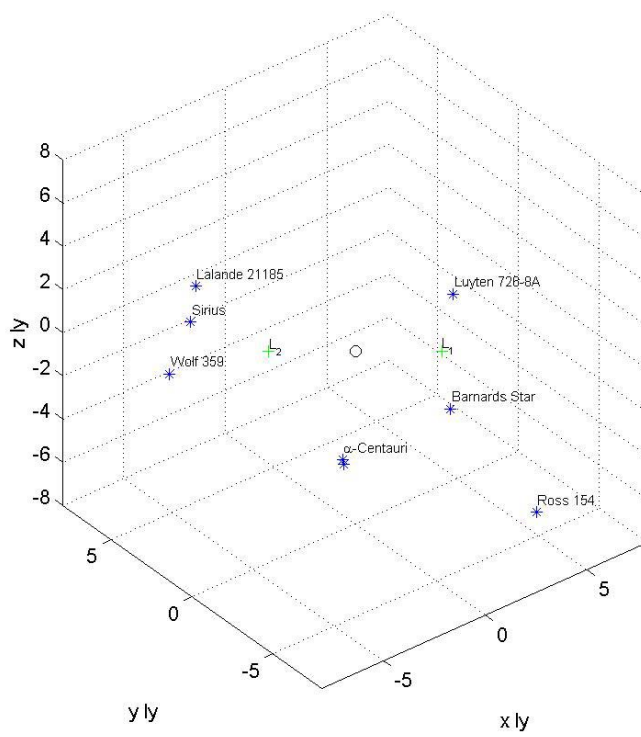


Figure 3.3.2 Stars within 3 pc of the Sun including L_1 and L_2

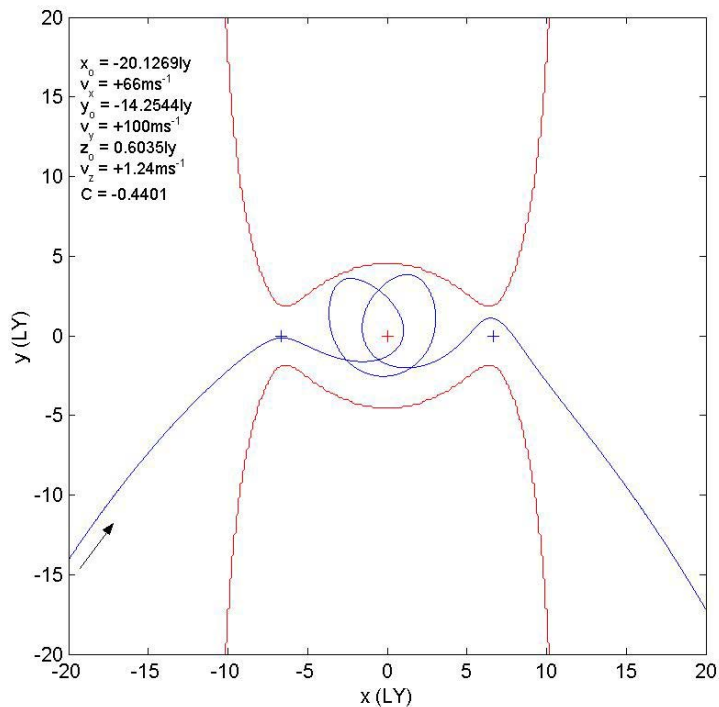


Figure 3.4.1 Transfer from interior to exterior Galactic region via L_1 and L_2

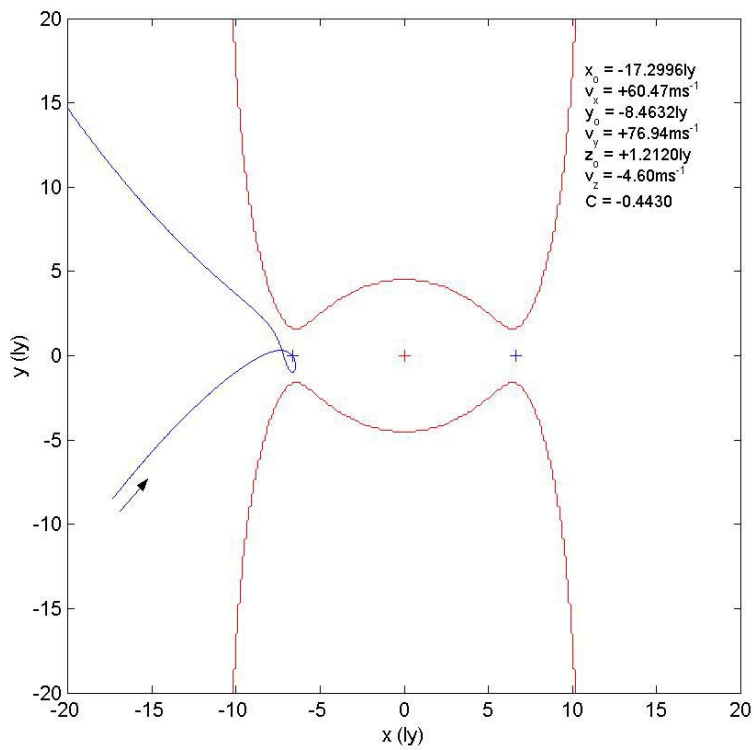


Figure 3.4.2 Lissajous orbit around L_1

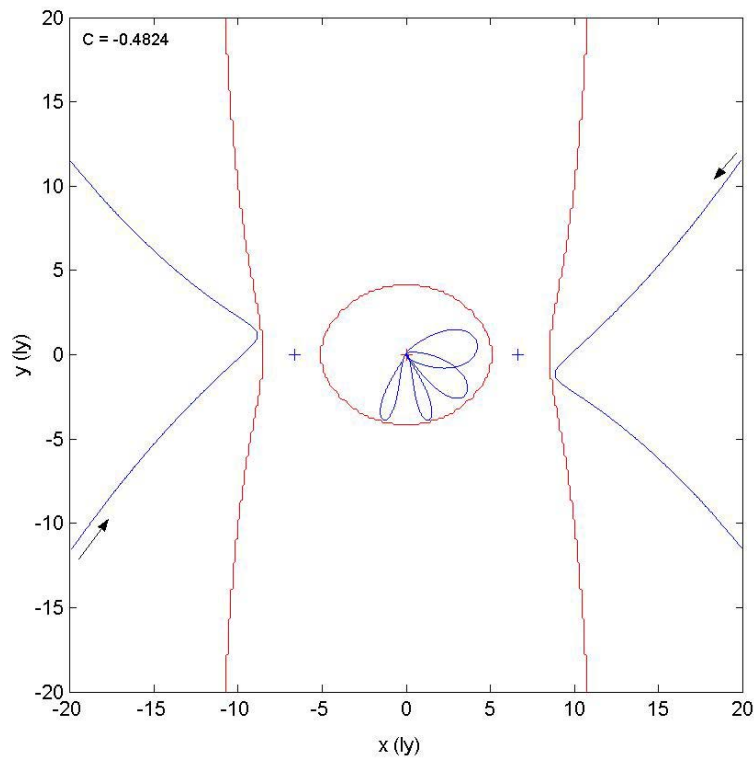


Figure 3.4.3 Closed zero velocity surface

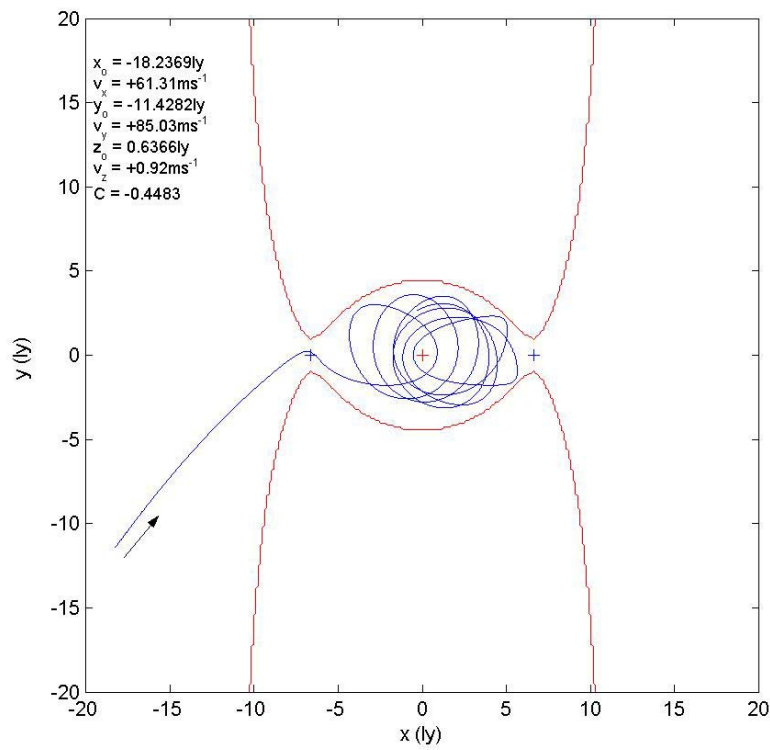


Figure 3.4.4 Capture from interior region via L_1

4. Libration Point Transfer for Interstellar Travel (WP3000)

4.1 Two-Centre Transfers

Orbit transfers via gravitational libration points are known to reduce the required energy compared to traditional transfer methods, such as Hohmann transfers. The transfer of a spacecraft between the Sun and Centauri will be investigated using the two-centre approximation. It has already been shown that the two-centre problem does not normally accurately model the dynamics of dust particles in the Sun–Centauri system, due to the relative motion of Centauri to the Sun. However, if a transfer takes a short period of time (~50 years) then the two-centre model is valid as the Centauri system can be assumed to be fixed relative to the Sun.

To traverse a distance of 4.36 ly in a period of 50 years would require a huge velocity of $26,159 \text{ kms}^{-1}$, 8.73% the speed of light. The relativistic effects on mass and time shall be ignored for this analysis. **Figure 4.1.1** considers a direct transfer departing from the Earth, positioned a distance of $1.49 \times 10^{11} \text{ m}$ from the Sun, and performs a fast-flyby at Centauri 50 years after launch. Due to the high-velocity, stellar gravity will not be sufficient to decelerate the probe adequately for capture, as the probe velocity is well in excess of the stellar escape velocity. The total energy applied to the spacecraft for this trip would be $3.4215 \times 10^{11} \text{ kJ/kg}$.

A much longer duration transit via the two-centre libration point is provided in **Figure 4.1.2**. The total transit time between the Sun and α -Centauri is 30 Myrs. Although the total mission energy requirement is -19.776 kJ/kg , much less than for the fast transfer case, the mission duration is clearly much too long. Due to the motion of Centauri relative to the Sun, this model has been shown to be invalid over such a long period of time.

4.2 Explicit Solution to Two-Centre Problem using Confocal Elliptical Coordinates

The two-centre problem can be solved explicitly by converting **Equation 1** to confocal elliptical coordinates ξ , η and θ (see **Appendix 1** for method).¹⁹ These equations are variable separable using the Hamilton-Jacobi method, allowing zero-velocity surfaces to be generated which may be used to identify bound motion in the two-centre problem. The separated equations are derived as

$$\begin{aligned} -8E\xi^2 + P_\xi^2(4\xi^2 - 1) + \frac{4P_\theta^2}{(4\xi^2 - 1)} - 8\xi(1 + \lambda) &= \alpha \\ 8E\eta^2 + P_\eta^2(1 - 4\eta^2) + \frac{4P_\theta^2}{(1 - 4\eta^2)} + 8\eta(1 - \lambda) &= -\alpha \end{aligned} \quad \text{Equation 14}$$

where P_ξ , P_η and P_θ represent the momentum terms, $\lambda=2.17$ is the ratio of m_1 to m_2 , E is the total energy and α is a separation constant.

From the initial conditions in polar coordinates, it is possible to calculate the initial values for $\xi, \eta, \dot{\xi}, \dot{\eta}$. Also, the values for energy and momenta can be determined, allowing the separation constant α to be calculated. Setting the values of P_ξ and P_η equal to zero, **Equation 14** can be solved to identify values of ξ and η representing zero-velocity surfaces for a set of initial conditions.

Figure 4.2.1 shows a set of ellipses which bound an orbit. The orbit in the ρ - z plane, represented by the bold line, is bound to the surface of an ellipse. It loops around the Sun and returns to the nominal orbit but never approaches Centauri. Applying an initial velocity alters the shape of the zero-velocity surface. **Figure 4.2.2** shows an orbit in the ρ - z plane, bound between two ellipses. This orbit loops around both the Sun and Centauri periodically.

Zero-velocity surfaces can be used to identify particle trapping orbits around a star. In the two-body problem a similar explicit solution exists by separating the equations of motion using parabolic coordinates.^{20,21} **Figure 4.2.3** shows an orbit where the particle has sufficient energy to escape the system. There are no surfaces bounding the particle to the two stars. Therefore, it can be concluded that the particle, in this case, can escape the two-centre system.

4.3 Mission Enabling Propulsion Systems

Transit times to Centauri prohibit the use of conventional propulsion methods. Instead a new, novel propulsion system will be required in order to conduct such a mission within a reasonable timescale. The suggested fast-flyby time of 50 years requires a huge energy of 3.4215×10^{11} kJ/kg and a cruise velocity of 8.73% of the speed of light. A selection of advanced propulsion concepts have been proposed which could reach relativistic speeds.

One such concept is solar sails, which are propelled by stellar radiation pressure. Acceleration is not limited by stored reaction mass so that solar sails could enable many exotic high-energy missions. For an interstellar mission, many engineering challenges would need to be overcome including deployment of a massive reflective structure in space and maintaining a flat surface. A very close solar pass at <0.01 AU (Astronomical Unit) could take advantage of the increased radiation pressure closer to the Sun, boosting the acceleration of the sail. Relying solely on stellar radiation pressure has the draw back that acceleration varies as $1/r^2$, where r is the distance from the star. Most of the 0.08 c velocity would have to be attained while the sail is within 1 AU of the Sun leading to a requirement for exotic, ultra-light sail materials.

Variations on the solar sail include the laser sail²² and maser sail²³, proposed by R. Forward. Both use extremely high-energy photon beams which can be focused onto a large reflecting structure, using a large diameter Fresnel zone lens. Since the beam is focused onto the sail, the $1/r^2$ dependence is removed and constant acceleration is in principle achievable. The advantage of beam power systems, in common with nuclear systems, is that the spacecraft arrives at the target power rich and capable of driving a substantial science payload. The clear disadvantage is the scale of engineering required for the power beam, and the total energy required to accelerate a large mass to mildly relativistic speeds. Engineering limitations exist regarding the thermal capacity of the material used for the sail. Forward states that a 65 GW laser could accelerate a 1000 kg sail with diameter 3.6 km at 0.036 g reaching Centauri within 40 years.

Figure 4.3.1 shows a selection of more exotic propulsion methods which have been suggested as propulsion systems enabling fast interstellar travel. No matter the propulsion system selected, we are required to consider exotic, speculative propulsion concepts. Indeed even nuclear electric propulsion is considered inadequate for true interstellar travel, due to the relatively low energy density of fission reactors. Eliminating the need for a reactor core and using the actual fission products as reaction mass is one way to attain higher energy densities.

The Orion concept, studied by NASA and others, proposed the use of pulse-propulsion for interplanetary and interstellar travel. Shown in **Figure 4.3.2**, a propulsive force could be produced by detonating fission devices behind the spacecraft with a pusher-plate mechanism driving the vehicle forward.²⁴

The use of anti-matter could enable high-energy density propulsion systems. Current global production of antimatter is extremely low. However, sufficient quantities could be produced as part of a focused research program towards the demonstration of antimatter propulsion capabilities. Penn State University have designed a spacecraft (ICAN-II) which would use antimatter: Fission/Fusion drive (ACMF) for planetary missions within the solar system, see **Figure 4.3.3**.

Fusion concepts have also been proposed which offer greater energy density than fission driven propulsion. One issue is plasma confinement in order to sustain a fusion reaction with two principle schemes - inertial confinement fusion (ICF) and magnetic confinement fusion (MCF). The British Interplanetary Society performed a feasibility study of ICF propulsion for interstellar travel. The study, known as Daedalus, used a two stage ICF system transporting a 830 megaton payload. The spacecraft could achieve interstellar flyby with a Δv of 0.1c, requiring 4 years to accelerate. This study outlined the possibilities using fusion energy, but many issues remain unresolved before fusion becomes a viable propulsion method.

Other propulsion options include the Buzzard Interstellar Ramjet, which was proposed by the physicist R.W. Buzzard during the 1960s. The concept uses a large magnetic collector or scoop, which directs interstellar hydrogen particles into a compressor where the gas can then be used as fusion fuel. The idea was proposed to reduce spacecraft mass by collecting fuel as it travels, although it has recently been demonstrated that the drag of particle collection would likely be larger than the energy produced by the fusion reaction.²⁵

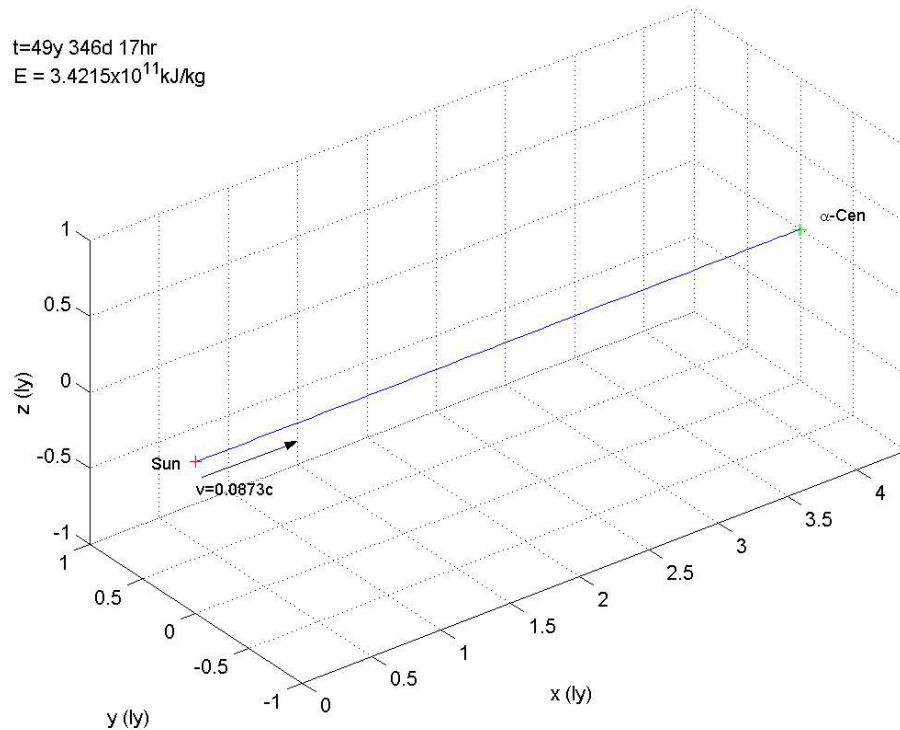


Figure 4.1.1 Space probe trajectory for fast-flyby of Centauri

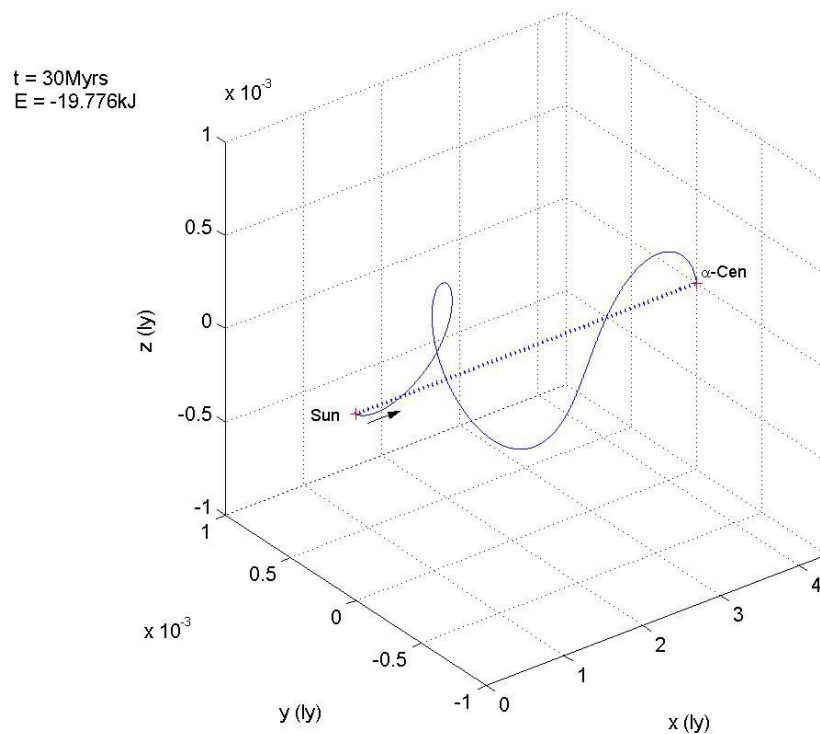


Figure 4.1.2 Long period transfer via libration point orbit

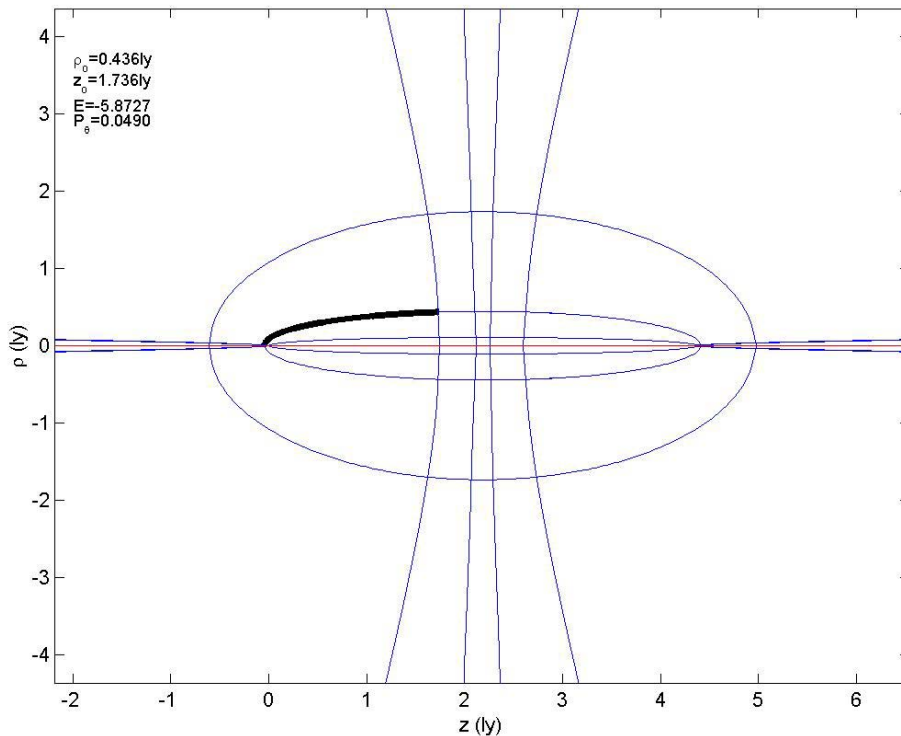


Figure 4.2.1 Elliptical coordinate bounding surface (Bold line represents orbit in ρ - z plane)

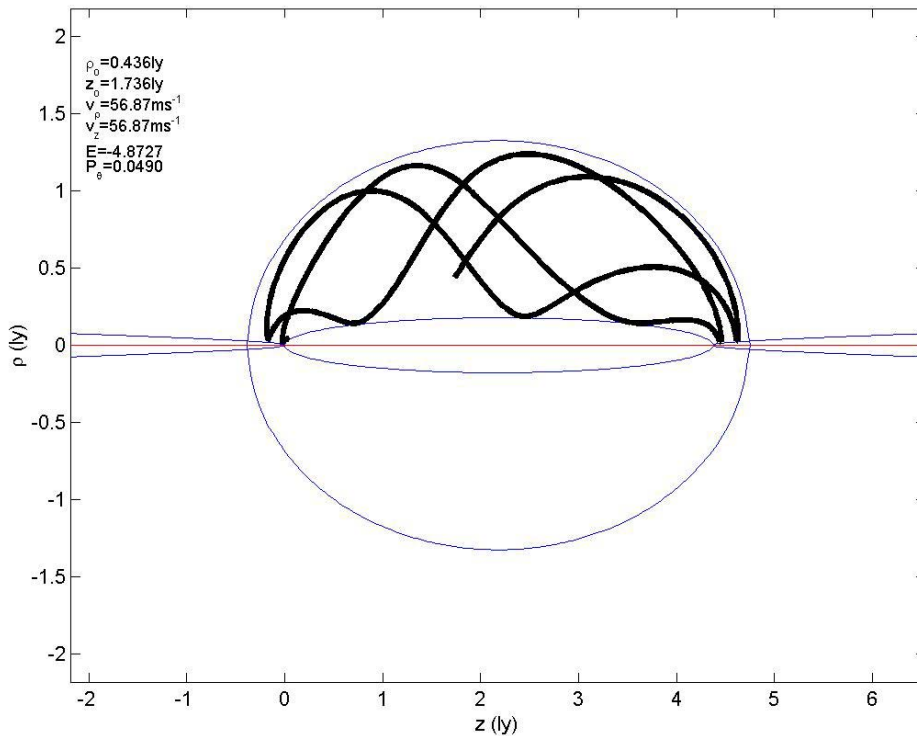


Figure 4.2.2 Elliptical coordinate bounding surface (Bold line represents orbit in ρ - z plane)

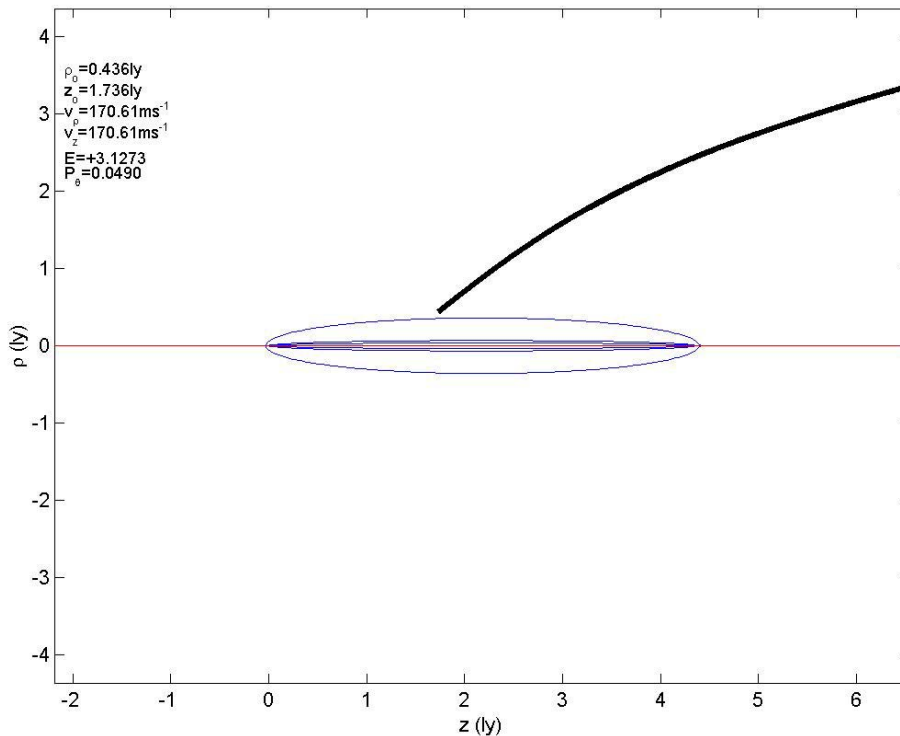


Figure 4.2.3 Escaping trajectory with no bounding ellipse

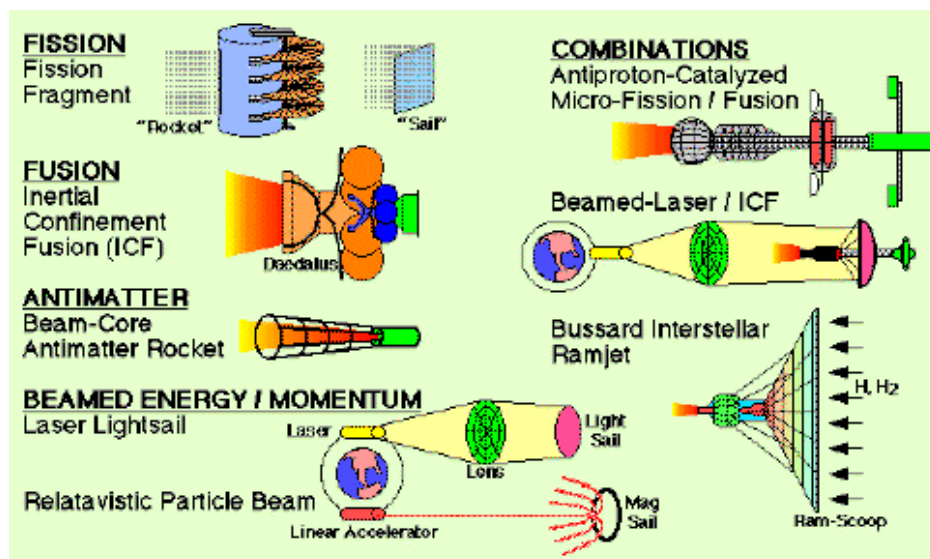


Figure 4.3.1 Candidate Interstellar propulsion systems (NASA/JPL)

Libration Points of the Sun and Interstellar Medium

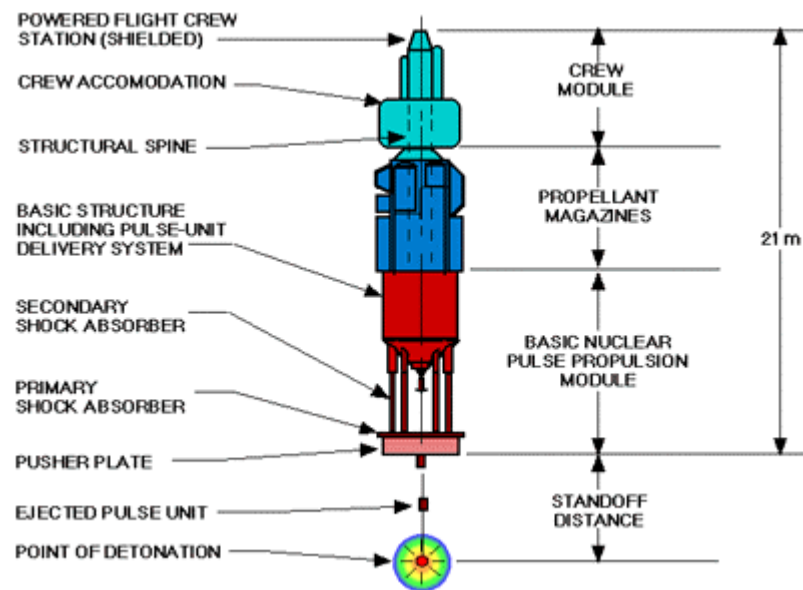


Figure 4.3.2 Orion concept for pulsed propulsion (NASA/JPL)

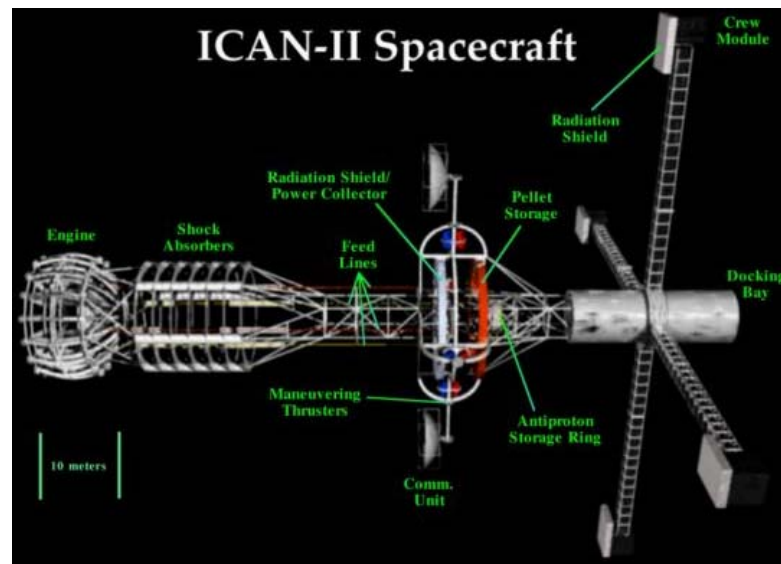


Figure 4.3.3 ICAN-II spacecraft (Penn State University)

5. Summary and Conclusions

The purpose of this study was to investigate dynamics of the Sun and the Centauri system and search for the location of possible libration points. The stability of such points was determined and the probability of interstellar matter becoming trapped, at least temporarily at these points, was addressed. The two-centre problem was used to model the dynamics of a test particle between the Sun and the Centauri system, making the assumption that the stars remain at fixed positions relative to each other. The on-axis libration point between the stars was identified and is located 1.76 ly from the Sun and 2.59 ly from Centauri. Using potential energy analysis, this libration point is seen to be unstable. Periodic orbits exist at various positions between the stars and there exist stable orbits near both the Sun and Centauri, corresponding to two-body orbits with a small uniform force displacing the orbits slightly from the nearby star. The typical orbit period was however found to be of order of 10 Myrs.

A study was also performed to examine the influence that stellar radiation pressure has on particles between the two stars using a new photo-gravitational two-centre problem. It was found that light extinction, due to scattering and absorption of photons by interstellar matter, does not significantly reduce the stellar luminosity at the on-axis libration point position. Therefore, stellar radiation pressure can have an effect on small particles at the libration points. A range of possible orbits were identified for different particle mass-to-area ratios.

To investigate the validity of the two-centre model, the effect of the motion of Centauri relative to the Sun was examined. It was found that Centauri moves fast relative to the Sun, compared to the timescale of the dynamics of the two-centre problem. Over a few hundred years the motion is barely noticeable, but after the 10 Myrs orbit period of typical two-centre orbits Centauri is distant from the Sun. It can be concluded that the two-centre model is normally not applicable to local stellar dynamics, as the stars move at relative speeds which are fast compared to the natural timescale of the dynamics of the problem. Therefore, no particles can be expected to become trapped at the transient libration points between the stars. The motion of nearby stars does however perturb the motion of test particles passing near the star. If a particle is moving away from the Sun at slightly greater than the solar escape speed, its energy can be reduced if it passes near Centauri, allowing it to be re-captured by the Sun.

The effect of a third potential, that of the binary system Sirius, was also included in the two-centre model and the potential energy function examined to search for libration points. It was found that the unstable libration point between the Sun and Centauri is still present, but that

another unstable libration point exists between the Sun, Centauri and Sirius. Again, photo-gravitational effects were included in this model.

The Sun orbiting the Galactic centre was modeled using Hill's approximation of the three-body problem. The L_1 and L_2 Lagrange points were identified at ± 6.64 ly and were found to be unstable using eigenvalue analysis. The position of all stars within 3 pc of the Sun were compared to the L_1 and L_2 position. Sirius was within 3.2 ly of L_2 and the red dwarf Barnard's star was within 2.75 ly of L_1 . These stars could significantly perturb any particles in the vicinity of the libration points.

Zero-velocity surfaces were generated for various particle energies using the Jacobi integral. Transfers between the interior Galactic region to the exterior region via the libration points were investigated. Also, cases where particles from the interior Galactic region can become captured were investigated. Although the period of these transfers is of the order of 100 Myrs, there is a possibility that interstellar matter transfers between the interior and exterior Galactic regions via this route.

Finally, transfers between the Sun and Centauri were investigated to outline a possible interstellar mission. Two possible missions were compared, a fast-flyby taking less than 50 yrs and a slow transfer using the two-centre libration point. The fast-flyby mission has a huge energy requirement of 3.4215×10^{11} kJ/kg and has a relativistic cruise speed of 0.0873 c. Using the two-centre libration point, a transfer requiring only -19.776 kJ/kg is found but with a period of 30 Myrs. Unfortunately, due to the motion of Centauri relative to the Sun, the transfer period is far too long for the two-centre model to be a valid approximation of the dynamics. Fast-flyby mission enabling propulsion systems were also investigated with a requirement for exotic high-energy density propulsion methods. The development of fusion and anti-matter driven systems could provide the huge amounts of energy required to traverse interstellar distances in a reasonable timescales.

6. References

¹ Howard, J.E., Wilkerson,T.D., 'Problem of two fixed centres and a finite dipole: A unified treatment', Physical Review A, Volume 52, number 6, Dec 1995, pp 4471-4492

² Nasa NStars Database, Ames Research Centre, California, 1988
<http://nstars.arc.nasa.gov/index.cfm>

³ McInnes, C, 'Solar Sailing Technology, Dynamics and Mission Applications', Springer-Praxis Series in Space Science and Technology, Springer-Verlag, Berlin, 1999, ch2

⁴ Scheffler, H, Elsässer,H, 'Physics of the Galaxy and Interstellar Matter', Springer-Verlag, Berlin, Heidelberg, 1988, Ch 1

⁵ Bertin, G, 'Dynamics of Galaxies', Cambridge University Press, 2000, Ch 2

⁶ Henry, R.C., 'The Local Interstellar Ultraviolet Radiation Field', The Astrophysical Journal, 2002, May, pp 697-707

⁷ Centre de Données Astronomiques de Strasbourg, VizieR Service, Nearby Stars, Preliminary 3rd Version (Gliese+ 1991), <http://cdsweb.u-strasbg.fr/viz-bin/VizieR?-source=V/70A>

⁸ Chandra X-ray Observatory, Operated for NASA by the Smithsonian Astrophysical Observatory, <http://www.chandra.harvard.edu>

⁹ Farquhar, R.W., 'The Flight of ISEE-3/ICE Origins, Mission History and a Legacy', J Astronautical Sciences, Vol 49, No.1, Jan-Mar 2001 pp23-73

¹⁰ Koon, W.S., Lo, M.W., Marsden, J.E., Ross, S.D., 'Low Energy Transfer to the Moon', Celestial Mechanics and Dynamical Astronomy Vol 81, 2001, pp63-73

¹¹ Franz, H. et al, 'WIND Nominal Mission Performance and Extended Mission Design', J Astronautical Sciences, Vol 49, No. 1, Jan-Mar 2001 pp145-167

¹² Fleck, B, Domingo, V, 'The SOHO mission', Kluwer Academic Publishers, c1995

¹³ Zhao, H, et al, 'Microlensing by the Galactic Bar', ApJ, 440, L13-L16, 1995, Feb 10

¹⁴ Ninković, S, 'On the Star Orbits in the Milk-Way Bulge', Serb. Astron. J, No 161, 2000, 1-3

¹⁵ Blum, R.D., 'Figure Rotation and the Mass of the Galactic Bulge', astro-ph/9503046, Mar 1995

¹⁶ Scheeres, D.J., 'Analysis of Orbital Motion Around 433 Eros', J of Astronaut. Sci., Vol 43, No.4 Oct-Dec 1995 pp427-452

¹⁷ Villac,B.F., Scheeres, D.J., 'Escaping Trajectories in the Hill Three-Body Problem and Applications', J Guidance Control and Dynamics, Vol 26, No.2, Mar-Apr 2003

¹⁸ Masdemont, J, Cobos, J, 'Astrodynamical Applications of Invariant Manifolds Associated with Collinear Lissajous Libration Orbits'

¹⁹ Waalkens, H, et al, 'Quantum Monodromy in the two-centre problem', J Phys. A:Math. Gen, Vol 36, 2003, pp307-314

²⁰ Burns, R.E., 'Motion of an Artificial Satellite under combined influence of planar and Keplerian force fields, NASA Tech Note, NASA TN D-4622, George C. Marshall Space Flight Centre, Huntsville, Ala., July 1968

²¹ Howard, J.E., 'Saddle-point Ionisation and the Runge-Lenz invariant', Physical Review A, Vol 51, No. 5, May 1995

²² Forward R.L., 'Roundtrip Interstellar Travel Using Laser-Pushed Lightsails', J. Spacecraft, Vol 21, No.2, Mar-Apr 1984, pp187-195

²³ Forward R.L., 'Starwisp: An Ultra-Light Interstellar Probe', J. Spacecraft, Vol. 22, No.3, May-June 1985, pp345-350

²⁴ Advanced Propulsion Concepts website, prepared by the Advanced Propulsion Technology Group, JPL, California Institute of Technology, Pasadena, California

<http://www.islandone.org/APC/index.html>

²⁵ Millis, M.G., Nasa Glenn Project Manager, Breakthrough Propulsion Physics Project, public information website <http://www.lerc.nasa.gov/WWW/PAO/html/warp/>

Appendix 1

The derivation of the explicit solution to the unequal mass two-centre problem is provided using confocal elliptical coordinates (ξ, η) . From Equation (1) we can define

$$(1) \quad r_1^2 = \rho^2 + z^2 = (\xi + \eta)^2$$

$$(2) \quad r_2^2 = \rho^2 + (1-z)^2 = (\xi - \eta)^2$$

so that

$$(3) \quad z = 2\xi\eta + \frac{1}{2}$$

$$(4) \quad \rho^2 = \frac{1}{4}(4\xi^2 - 1)(1 - 4\eta^2)$$

We find the derivatives of (3) and (4) with respect to time as

$$(5) \quad \dot{z} = 2\dot{\xi}\eta + 2\xi\dot{\eta}$$

$$(6) \quad \dot{\rho} = \frac{\xi\dot{\xi}}{\rho}(1 - 4\eta^2) - \frac{\eta\dot{\eta}}{\rho}(4\xi^2 - 1)$$

The Hamiltonian $H = T + U$ is now defined where T is the kinetic energy and U is the potential energy. For the two centre problem, the Hamiltonian in polar coordinates maybe written as

$$(7) \quad H = \frac{1}{2}(\dot{\rho}^2 + \dot{z}^2 + \rho^2\dot{\theta}^2) - \frac{1}{r_1} - \frac{\lambda}{r_2}$$

Equation (7) can be re-written in elliptical coordinates using (5) and (6) to obtain

$$T = \frac{1}{2} \left[4\dot{\xi}^2 \left(\xi^2 \frac{(1 - 4\eta^2)}{(4\xi^2 - 1)} + \eta^2 \right) + 4\dot{\eta}^2 \left(\eta^2 \frac{(4\xi^2 - 1)}{(1 - 4\eta^2)} + \xi^2 \right) + \frac{1}{4} (4\xi^2 - 1)(1 - 4\eta^2) \dot{\theta}^2 \right]$$

from which we can obtain the momenta terms P_ξ , P_η and P_θ

$$\begin{aligned}
 P_\xi &= \frac{\partial T}{\partial \dot{\xi}} = 4\dot{\xi} \left(\xi^2 \frac{(1-4\eta^2)}{(4\xi^2-1)} + \eta^2 \right) \\
 P_\eta &= \frac{\partial T}{\partial \dot{\eta}} = 4\dot{\eta} \left(\eta^2 \frac{(4\xi^2-1)}{(1-4\eta^2)} + \xi^2 \right) \\
 P_\theta &= \frac{\partial T}{\partial \dot{\theta}} = \rho^2 \dot{\theta}
 \end{aligned}$$

Then the Hamiltonian can be written in elliptical coordinates as

$$(8) \quad H = \frac{1}{2} \left(\frac{P_\xi^2 (4\xi^2 - 1)}{(4\xi^2(1-4\eta^2) + 4\eta^2(4\xi^2-1))} + \frac{P_\eta^2 (1-4\eta^2)}{(4\xi^2(1-4\eta^2) + 4\eta^2(4\xi^2-1))} + \frac{P_\theta^2}{\rho^2} \right) - \frac{1}{(\xi + \eta)} - \frac{\lambda}{(\xi - \eta)}$$

A common factor of $1/(4(\xi^2 - \eta^2))$ can be identified in (8) to yield

$$(9) \quad H = \frac{1}{8(\xi^2 - \eta^2)} \left[P_\xi^2 (4\xi^2 - 1) + P_\eta^2 (1-4\eta^2) + 4P_\theta^2 \left(\frac{1}{(4\xi^2-1)} + \frac{1}{(1-4\eta^2)} \right) \right] + \frac{\eta(1-\lambda) - \xi(1+\lambda)}{(\xi^2 - \eta^2)}$$

Then the Hamilton-Jacobi transforming function S can be used to separate the variables as

$$(10) \quad S = -Et + P_\theta \theta + S(\xi) + S(\eta)$$

where t is the time and E is the total energy. For certain values of S, it is true that

$$\frac{dS}{dt} + H = 0, \text{ therefore}$$

$$-E + \frac{1}{8(\xi^2 - \eta^2)} \left[P_\xi^2 (4\xi^2 - 1) + P_\eta^2 (1-4\eta^2) + 4P_\theta^2 \left(\frac{1}{(4\xi^2-1)} + \frac{1}{(1-4\eta^2)} \right) \right] + \frac{\eta(1-\lambda) - \xi(1+\lambda)}{(\xi^2 - \eta^2)} = 0$$

Re-arranging we obtain

$$(11) \quad -8E\xi^2 + 8E\eta^2 + P_\xi^2 (4\xi^2 - 1) + P_\eta^2 (1-4\eta^2) + \frac{4P_\theta^2}{(4\xi^2-1)} + \frac{4P_\theta^2}{(1-4\eta^2)} - 8\xi(1+\lambda) + 8\eta(1-\lambda) = 0$$

where (11) can be separated into two expression with separation constant α

$$-8E\xi^2 + P_\xi^2(4\xi^2 - 1) + \frac{4P_\theta^2}{(4\xi^2 - 1)} - 8\xi(1 + \lambda) = \alpha$$

$$8E\eta^2 + P_\eta^2(1 - 4\eta^2) + \frac{4P_\theta^2}{(1 - 4\eta^2)} + 8\eta(1 - \lambda) = -\alpha$$

as defined in Section 4.2.